RECORD No. 1966/154

GOULD AREA GEOCHEMICAL AND GEOPHYSICAL SURVEYS, RUM JUNGLE AREA, NORTHERN TERRITORY 1965

by

D.O. SHATWELL and K. DUCKWORTH

CONTENTS

ILLUSTRATIONS

SUMMARY

Reconnaissance geological, geochemical, and geophysical surveys were made in an area to the south of Batchelor, Northern Territory, during 1965 by the Darwin Uranium Group of the Bureau of Mineral Resources. Traverses spaced 2400 feet apart were sampled every 400 feet by auger drilling in areas of soil cover and by mattock sampling in areas of outcrop. The samples were analysed for copper, lead, nickel, cobalt, vanadium, and phosphorous by Australian Mineral Development Laboratories, Adelaide. Geochemical results from the auger samples were considered to be equivalent to those from mattock samples as both were taken from residual material overlying weathered rock. All auger holes were radiometrically probed.

The geophysical work consisted of electromagnetic and surface radiometric readings along the traverses spaced at 2400-ft intervals. The results were compared with geochemical and geological data in evaluating possible mineralisation. These surveys outlined an area of interest near the Waterhouse No. 2 Prospect and extending north of Mount Minza. In this area intense electromagnetic anomalies are associated with radiometric and weak geochemical anomalies. Geological mapping showed that the succession at Mount Minza is similar to that at the Waterhouse No. 2 Prospect - an important consideration as uranium mineralisation and traces of copper are known from previous surveys at Waterhouse No. 2.

Follow-up geochemical and geophysical surveys were commenced in the anomalous areas on a 200 x 400-ft grid. This work was designed to cover the major electromagnetic anomalies but did not include all geochemical anomalies.

The electromagnetic results obtained in the field were compared with results from laboratory experiments on model conductors. A quantitative estimate of the position, depth, width, and dip of the conducting bodies at Mount Minza was computed and is used as an aid to siting two proposed diamond-drill holes.

A programme for 1966 is suggested, in which the area of detailed coverage is extended to the north, west, and south to cover all geochemical anomalies. The results of the reconnaissance survey do not warrant any further work in the remainder of the Gould area.

1. INTRODUCTION

Geological, geochemical, and geophysical surveys of an area known as the Gould area were made by geological and geophysical parties of the Darwin Uranium Group of the Bureau of Mineral Resources (BMR) as part of their 1965 field programme. The technique of using these methods on widely spaced traverses was adopted as it enables the mineral potential of a relatively large area to be assessed rapidly, so that anomalous areas may be subsequently investigated in more detail.

The Gould area is of interest because the Coomalie Dolomite and the Golden Dyke Formation, hosts for mineralisation in other parts of the Rum Jungle district, pass through it, and because of a number of known mineral prospects. Most of the known mineralisation in the Rum Jungle field is localised close to the contact between the two formations.

Base metal and uranium mineral deposits were sought by geological mapping and radiometric, geochemical, and geophysical surveys using the same base grid. The surveys were aimed at delineating broad zones of possible mineralisation and at establishing the geology in areas of soil cover. It was planned to follow up the work in 1966 by examining in detail any mineralised zones.

This report describes the work carried out jointly by the geological and geophysical field parties. The sections on geology and geochemistry were written by D.O. Shatwell and those on geophysics by K. Duckworth.

Work was commenced in June 1965, and completed in November 1965.

Situation and access

The survey area is situated south of the township of Batchelor and lies between the eastern margin of the Waterhouse Granite and the Stuart Highway as shown in Plate 1. The area measures approximately 4½ miles by 6 miles, the northern section lying in the Hundred of Goyder and the remainder in the Hundred of Waterhouse. The North Australian Railway approximately bisects the area in a north-south direction, and a number of dry-weather tracks provide access.

Surveying

Traverses spaced 2400 feet apart and pegged at 50-ft intervals provided a basic grid for the reconnaissance work. A surveyor under contract to the Department of the Interior carried out the surveying. The grid co-ordinates are based on the mine grid of Territory Enterprises Pty Ltd (T.E.P.).

A baseline, bearing 359°58'00" True, was established along co-ordinate 38,000E of the mine grid. The azimuth of the baseline was derived from the known direction of a line joining Stratton Trig Station to 65B Trig Station, and the co-ordinates of the latter, obtained from T.E.P., were used to derive the co-ordinates of the Gould area.

Additional traverses in the Mount Minza area, were pegged by the geophysical party for more detailed work.

For the sake of brevity, traverses have been numbered according to the mine grid co-ordinates along which they were made, but with the final two zeros deleted, eg. traverse 213S is along co-ordinate 21,300S.

Methods used

The geological party, consisting of D.O. Shatwell, A. Wiriasumita (geologists), an auger driller and assistant, and two field-hands, carried out auger drilling, geochemical sampling, geological mapping, and

radiometric probing of auger holes.

The geophysical party, consisting of K. Duckworth (geophysicist), C.J. Braybrook (geophysical assistant), and two field-hands, was concerned with electromagnetic, surface radiometric, and magnetic surveys.

2. PREVIOUS WORK IN THE AREA

The geology of the Darwin/Adelaide River area, which includes the Gould area, has been described by Malone (1958). Airborne radiometric surveys made by the BMR in 1952 and 1957 located a number of radiometric anomalies (Wood & McCarthy, 1952; Livingstone, 1959). As a result of the 1952 airborne survey, four areas of anomalous radioactivity within the present survey area were selected for follow-up work by ground parties. These areas are known as Area 65 (formerly Waterhouse No. 1) Prospect and Waterhouse Nos. 2, 3, and 4 Prospects.

Area 65 (Waterhouse No. 1) Prospect

Although this prospect lies just within the Gould area, the 1965 survey provided no additional information on it. Previous work includes geological mapping, geochemical sampling, radiometric, magnetic, and self-potential surveys, and diamond drilling, carried out between 1953 and 1961 (Rosenhain & Alle, 1953; Daly & Tate, 1958; Douglas, 1962; Ruxton & Shields, 1963). The surveys outlined a zone of copper anomalies with weak surface copper mineralisation, coinciding with a Turam anomaly and a small radiometric anomaly. Diamond drilling did not reveal any economic mineralisation at depth.

Waterhouse No. 2 Prospect

A preliminary geological, radiometric, geochemical, and magnetic survey (Wyatt & Alle, 1953) revealed copper and radiometric anomalies. The area was held under reserve by Northern Uranium Development, N.L.; this company sank a shaft to 41 feet, drilled a diamond-drill hole and bulldozed ten costeans. Uranium mineralisation, apparently approaching ore grade, was intersected over a few feet in the shaft. An electromagnetic survey and some magnetic and gravity work were carried out in 1957 (Daly & Tate, 1960). Five diamond-drill holes were recommended to test the electromagnetic indications, and two were subsequently drilled. Results of the diamond drilling are described by Ruxton (1961) who reported anomalous radioactivity in black slates in one of the holes. He also recorded phosphate (apatite crystals in amphibolite) in a second hole. No further work has been done to test the uranium mineralisation in the shaft.

Waterhouse No. 3 and 4 Prospects

Radiometric and magnetic surveys carried out by Alle (1953a & b) and electromagnetic traverses (Daly & Tate, 1960) suggest that the anomalies in these two areas are due to superficial causes only. No. 3 Prospect is in radioactive siltstone rubble, and No. 4 in laterite. Daly & Tate do not consider that either prospect warrants further investigation.

Phosphate investigations

Phosphate mineralisation at Stapleton North was investigated by P.W. Pritchard of the BMR in 1963 (pers. comm.). A number of percussion holes and one diamond-drill hole apparently did not intersect ecomonic phosphate at depth.

3. RECONNAISSANCE SURVEY

Physiography

The Gould area may be divided into two broad physiographic units:

(1) A low-lying area of mature topography and subdued relief occupying the central part of the area.

(2) Areas of dissected strike ridges and hilly country bordering the first unit to the east, west, and south.

The transition from mature to dissected topography is fairly abrupt and is caused by resistant beds in the latter areas, principally quartzite, quartzite breccia, and greywacke to the east and south and conglomerate and breccia to the west.

The dissected areas rise about 100 feet above the general level; the highest point, Mount Minza, is approximately 300 feet above this level. Generally the summit levels are uniform, suggesting an earlier peneplanation, perhaps corresponding to that preserved elsewhere at the base of the Cretaceous.

Drainage is principally to the west, into the Finniss River, and to the south-east, via Stapleton Creek, into the Adelaide River.

Stratigraphy

The stratigraphic nomenclature adopted in this record is based on that of the Rum Jungle 1 inch to 1 mile geological map published by the BMR in 1960.

The following units were recognised and mapped in the Gould area (Plates 2 & 3):

Superficial deposits	(Quaternary)
Laterite	(? Tertiary)
Amphibolite	(? Lower Proterozoic)
Noltenius Formation	(Lower Proterozoic)
Acacia Gap Tongue of the Masson Formation	(Lower Proterozoic)
Golden Dyke Formation	(Lower Proterozoic)
Coomalie Dolomite	(Lower Proterozoic)
Crater Formation	(Lower Proterozoic)

Most of the above units have been described on a regional basis by Malone (1958), so that the following remarks are concerned with observations in the Gould area only.

Crater Formation. The Crater Formation forms a well-defined SSE-trending ridge on the western margin of the area. It consists chiefly of hematitic and quartz-hematite conglomerate, sheared arkose and arkosic grit, quartzite and quartz-rich breccia, and quartz-tourmaline rocks. In general the formation is more ferruginous in the northern and more siliceous in the southern sections. A highly generalised geological section of the formation may be compiled, in descending stratigraphic order, as follows:

Quartz-tourmaline rocks

Arkose, arkosic grit

Conglomerate, quartzite, quartzite breccia

Hematitic conglomerate.

Thus the more hematitic rocks occur near the base of the formation and are overlain by the more siliceous and tourmaline-rich types. The tourmaline-bearing rocks comprise the most common and persistent unit of the formation, and fall into three categories: (a) banded quartz-tourmaline types, which appear to be reconstituted sediments, (b) partly to completely tourmalinised arenites, and (c) quartz-tourmaline vein material.

A lens of highly hematitic rock thought to be a conglomerate crops out in the northern part of the area. It consists of closely packed ovoid bodies up to 1 foot long, composed of quartz and specular hematite, resembling flattened boulders. The direction of flattening defines a rough foliation. One of the hematitic bodies assayed 33.6% iron.

Probably much of the hematite in the sediments was deposited at the time of sedimentation; but this cannot be true of the tourmaline, which must have been introduced and concentrated by metasomatism. According to Rhodes (1964) the Rum Jungle complex contains late-stage intrusive phases; it is suggested here that such an intrusive phase in the Waterhouse Granite, which the Crater Formation unconformably overlies, could have caused introduction of boron sufficient to account for the tourmaline in the Crater Formation.

Coomalie Dolomite. Most of the area mapped as Coomalie Dolomite is soil covered, and auger drilling disclosed only deep quartz sand in a ferruginous or kaolinitic matrix. Elsewhere at Rum Jungle this sand is known to overlie dolomite, and its occurrence in the Gould area is accepted as evidence of Coomalie Dolomite.

In the north-west part of the area, lenticular bodies of ferruginous breccia and vuggy quartzite are exposed in the Coomalie Dolomite. The breccia consists of angular quartz fragments in a limonitic or hematitic matrix, and is designated as "dolomitic breccia" in Plate 2. It is commonly associated with a fine- to coarse-textured quartzite which has a somewhat calcareous aspect on weathered surfaces.

No unaltered dolomite was noted in the Gould area.

Golden Dyke Formation. The Golden Dyke Formation occupies the major part of the Gould area and is well exposed on the eastern side. Shale and siltstone, commonly silicified, are the dominant lithologies, but lenses of quartzite, carbonaceous and graphitic shale, chloritic and sericitic schist, greywacke, chert, breccia, limestone, and tremolitic siltstone are also present. The formation is extensively intruded by amphibolite.

The lowermost beds are not well exposed, but consist predominantly of shale, siltstone, and a few beds of quartzitic breccia. Some of these breccia beds are shown as Coomalie Dolomite in the Rum Jungle 1 inch to 1 mile geological map published by the BMR in 1960, probably because they resemble a weathered carbonate.

Beds of carbonaceous and graphitic shale, chlorite schist, and chlorite-sericite schist, mostly adjacent to amphibolite, are common in the middle section of the formation. These are associated with beds

of tremolitic siltstone, hematitic quartz breccia, and banded ironstone, which are folded into a south-plunging anticline in the area between Mount Minza and the Waterhouse No. 2 Prospect. The carbonaceous and graphitic shale and chlorite schist apparently lens out on the eastern limb of this anticline, but the hematitic quartz breccia and banded ironstone persist and form a prominent SSW-trending ridge on the eastern side of the area. The uppermost beds in the Golden Dyke Formation are somewhat more cherty and are probably a transitional phase of the Burrel Creek Formation. Beds of blocky chert and thin bands of quartzite are common.

The geology of the Mount Minza/Waterhouse No. 2 area is described in detail in a later section.

Acacia Gap Tongue. The Acacia Gap Tongue of the Masson Formation crops out as a thin pyritic quartzite bed within the Golden Dyke Formation, in the north-eastern sector of the Gould area. This unit lenses out to the south.

Noltenius Formation. The Noltenius Formation lies in the south-eastern corner of the Gould area and is well exposed in moderately rugged topography. The typical lithology is grey or buff medium-grained subgreywacke, but lenses of blue-grey siltstone and coarser phases of grit and conglomerate occur. Typically the rocks contain up to 50% quartz grains, 25 to 50% quartz-sericite matrix, and about 10% rock fragments. The rock fragments are either cherty or consist of material similar in composition to the matrix. Felspar is rare, and tourmaline is a constant accessory mineral. Hematite is commonly present, either in the form of separate grains or as a constituent of the matrix.

The acid nature of the rock and rock fragments and the presence of tourmaline indicate that the formation could have been derived originally from a granitic source - possibly the Crater Formation or its equivalent. If this is the case, the Golden Dyke/Noltenius Formation boundary may be an unconformity. Some evidence for this is provided by the localised distribution of the formation, and by the fact that conglomerate lenses occur close to the boundary with the Golden Dyke Formation.

Amphibolite. Amphibolite bodies form a broad, north-easterly trending zone within the Golden Dyke Formation, approximately parallel to the regional strike. Amphibolite has also been mapped close to the Coomalie Dolomite/Golden Dyke Formation boundary on traverses 141S, 165S, and 189S, and in the north-western part of the area on traverse 21S. The major north-easterly-trending body is the source of an aeromagnetic anomaly (BMR geophysical map No. G71-92A), apparently caused by magnetite in the amphibolite, although ground magnetic traverses failed to establish a detailed agreement between the distribution of amphibolite and magnetic anomalies. All the amphibolite bodies broadly coincide with a zone of disturbed Slingram values.

Amphibolite has been recorded in a diamond-drill hole at Waterhouse No. 2 Prospect (Ruxton, 1961) and is described as an igneous rock in an appendix to that Record by Bryan, partly because of the presence of apatite. Only one small outcrop was found containing approximately 75% tremolite, 10% chlorite, and 5% each of plagioclase, calcite, and magnetite. Accessory sphene is present, and apatite was not recognised. The hypidiomorphic texture under the microscope and the general appearance in hand specimens are those of an igneous rock.

Although broadly concordant with the regional strike, the amphibolite in places cuts across the strike of older rocks, suggesting that it is intrusive. This could only be substantiated by detailed auger drilling.

Amphibolite was mapped where green to khaki chloritic clay, generally containing calcareous concretions and magnetite, occurred in the auger cuttings. Well-foliated chlorite schist fragments in the clay in some cases suggest that amphibolite is either associated with, or alters to this material. Tremolite in siltstone, and chlorite in limestone, cropping out adjacent to amphibolite, are possibly metamorphic or meta-somatic minerals related to intrusion of the amphibolite.

The amphibolite body on traverse 21S has no aeromagnetic anomaly associated with it and no magnetite was recorded in auger cuttings of the overlying clay. Mapping by T.E.P. suggests that this body may be correlatable with one of the amphibolites in the embayment area, north of the Giant's Reef Fault (Plate 1).

Laterite. Laterite cappings are sporadically distributed over the Gould area. Typically, the laterite consists of ferruginous, nodular, or cellular concretionary bodies a few feet thick, generally with a level surface. In some places, fragments of quartz or underlying rock are incorporated in the laterite; the term 'ferricrete' has been applied by some authors to this material. In the Mount Minza area, laterite appears to be associated with fault traces; but selective emplacement of laterite over certain beds has also been inferred from the fact that, in one case, the laterite terminates at a fault trace.

Superficial deposits. The low-lying parts of the Gould area are covered by a mantle of superficial material of varying thickness. These deposits may be classified as follows:

(a) River gravels. River gravels occur in the north-west part of the area and are confined to areas underlain by Coomalie Dolomite. These deposits could not be auger drilled to any depth. The gravel deposits are estimated to exceed 10 feet in thickness and are composed of rounded siliceous pebbles up to 2 inches in diameter, associated with quartz sand.

(b) Humic swamp deposits. Two swamps in the south-western part of the area contain black soil. These were not auger drilled as the swampy nature of the soil renders them inaccessible to vehicles.

The swamps over-lie a possible fault trace in the Coomalie Dolomite.

(c) Residual and semi-residual soils. Most of the Gould area is covered by soils, which are divided into three zones, here called horizons A, B, and C (not all of which are everywhere present).

The A horizon consists of a mantle of grey humic soil a few inches to a foot thick; the B horizon is red-brown, ferruginous, and ranges in thickness from 0 to more than 50 feet; the C horizon consists of non-ferruginous clays and rock fragments, and in colour and composition generally reflects the nature of the underlying fresh rock.

The C horizon, and to a lesser extent the B horizon, were used in the survey to identify the nature of unexposed rock. In areas underlain by Coomalie Dolomite, the B horizon is much thicker than elsewhere (always greater than 20 feet), and it was not possible to penetrate it with the auger drill. It is composed of well-rounded and sorted quartz grains in a ferruginous, and in places kaolinitic, matrix.

The Golden Dyke Formation is overlain by a B horizon composed of ferruginous pisolites and ferruginised rock fragments; it is generally less than 20 feet thick and in places absent.

In the south-west part of the area the B horizon contains angular quartz gravels which could not be penetrated by the auger drill, and effectively obscured the underlying geology.

Structure

Folding. Most of the dips recorded in the Gould area are to the east and range from 30° to 70°, the sediments dipping off the eastern margin of the Waterhouse Granite. The only major modifying structure is an anticline in the Mount Minza area, plunging south to south-west.

The easterly divergence of the Golden Dyke Formation from the Crater Formation (and apparent thickening of the Coomalie Dolomite) in the northern part of the area, is undoubtedly of structural origin; the area may be regarded as a broad structural 'saddle' between the Rum Jungle and Waterhouse Granites.

Cleavage and small-scale folding are well developed in the more argillaceous sediments, and brecciation is common in siliceous sediments. The cleavage generally strikes north and is parallel to the major fold direction. The small-scale folds do not seem to bear this relationship to the main folding and are best developed where very thin siliceous beds are intercalated with shale in the Golden Dyke Formation, north-east of Mount Minza. Here the folds plunge to the south-east and display a clockwise sense of rotation. It is possible that they are associated with NE-trending faults, the axial planes of the small folds acting together with the fault planes as conjugate shears in response to east-west flattening.

Brecciation is generally found in narrow quartzitic beds intercalated with shale, suggesting that its origin is tectonic. However, it is possible that some of the breccias have been formed by slumping.

Faulting. Two prominent fault directions are recorded: major faults trending north-easterly, and small faults trending approximately northerly. The north-easterly fault system is prominent in the Mount Minza area, where several parallel faults occur. One of these apparently cuts off the western limb of a syncline conjugate with the major anticline in this area; movement appears to have taken place along a bed of hematitic quartz breccia where this breccia trends parallel to the major fault direction. Small pods of breccia have been 'stretched out' along the fault plane.

Faults can generally be inferred from brecciation and shearing along the fault trace. In some cases, displacement of electromagnetic anomalies is a criterion for faulting.

Auger drilling and geochemical sampling

Geochemical samples were collected along all traverses at intervals of 400 feet. Mattock samples were collected over areas of outcrop and residual rock debris. Auger holes were drilled, using a Gemcodrill, in areas of soil cover. The purpose of the auger drilling was threefold:

(a) to obtain a sample, preferably of weathered rock, for geochemical analysis;

(b) to determine the nature of the underlying rock;

(c) to measure radioactivity beneath transported overburden by radiometric probing.

All samples were submitted to the Australian Mineral Development Laboratories (AMDEL) for determination by optical emission spectrograph of copper, lead, nickel, cobalt, vanadium, and phosphorus.

In many cases it was not possible for the auger drill to penetrate to the C (or weathered rock) horizon, so that some samples were taken from clays of the B horizon. In order to estimate the effect of this procedure on analysis results, on two traverses a sample was collected from each soil horizon (A, B, and C) whenever these were intersected and clearly defined. On traverse 213S some of these samples yielded anomalous values and the analyses for copper, cobalt, and nickel are presented in profile form over the anomaly area (Plate 10). The high values are clearly defined in the B and C horizons but are flattened and somewhat smoothed in the A horizon. It is concluded, therefore, that for reconnaissance surveys in soil-covered areas, the values from the B and C horizons, which both consist of residual material, may be evaluated together; but that the A horizon should be treated separately. In areas of outcrop a mattock sample is considered to yield results comparable to those from the B and C horizons, which are, of course, not developed in such areas.

Most of the drilling was done by a Gemcodrill owned and operated by the BMR. Towards the completion of the work, however, some auger drilling was done by a contractor to Territory Enterprises Pty Ltd.

A total of 12,211 feet was drilled in the Gould area; the footages drilled by the two machines are as follows:

11,153 feet drilled by BMR

1,058 feet drilled by contractor.

Radiometric probing

Auger holes were probed for radioactivity using Harwell type 1368A ratemeters and probe units. The readings were recorded at one-foot intervals down the auger holes.

The aim of the probing was to determine radioactivity of residual soils of the B and C horizons, that is, below the mantle of transported material. For this purpose the maximum value in residual material for each auger hole was adopted, as the B and C horizons were considered to be equivalent. Anomalies which persist into the C horizon, however, may be more significant than those which do not.

The radiometric values are shown as profiles in Plates 6 and 7. Surface radiometric profiles have also been plotted from the values at each sample location for two reasons: firstly, for direct comparison with the subsurface readings; and secondly, so that the

subsurface profiles may be extended on to areas of outcrop that were not auger drilled and realted to the surface readings in these areas.

Instrument variation was minimised by checking the probe units twice daily against a standard hole and correcting the readings if necessary.

Results

Geochemical. Geochemical analysis results are tabulated in the appendices; areas of high metal values are shown in Plates 4 and 5.

A statistical analysis of the frequency distribution of the geochemical analysis values was carried out in order to attempt a division of the values into anomalous and background populations. The frequency distribution curves were plotted on logarithmic probability paper and are shown in Plate 11.

Most of the curves approximate to a single log-normal distribution modified by minor inflexions. It is difficult to distinguish between inflexions due to trivial causes and those that reflect the existence of separate background and anomalous populations, hence selection of a 'significant' value is largely a matter of intuition.

The following values have been selected as threshold:

Copper	100 p.p.m.
Lead	250 p.p.m.
Cobalt	300 p.p.m.
Nickel	300 p.p.m.
Vanadium	250 p.p.m.
Phosphorus	500 p.p.m.

Plates 4 and 5 illustrate areas in which the metal values exceed these figures. There are two anomalous zones: (a) a zone of high copper, nickel, and cobalt on traverses 237S and 261S, near the Waterhouse No. 2 Prospect, and (b) an extensive zone of high values associated with a south-plunging anticline to the north-east of (a). In the Mount Minza area copper, cobalt, nickel, vanadium, and phosphorus are anomalous; a few 'spot' lead anomalies are also present.

These two areas, though separate, are related geologically, and have the following characteristics in common:

(1) They occur in the Golden Dyke Formation, where carbonaceous and graphitic shale, hematitic quartz breccia, and amphibolite are the main rock types.

(2) They are associated with Slingram and Turam anomalies.

Because of the intensity of the electromagnetic anomalies, additional traverses were pegged, in most cases 400 feet apart. Auger and mattock samples were collected at intervals of 200 feet along these traverses and analysed for copper and cobalt by atomic absorption spectrograph. The aim of the additional work was to investigate the relationship of anomalies and geology between the two areas.

The geology and geochemistry of the Mount Minza/Waterhouse No. 2 subarea is described in greater detail in Chapter 4 of this Record.

Areas in which vanadium values exceed 250 p.p.m. probably indicate lithologies that are normally rich in this element, such as black shale or amphibolite. The zone of high vanadium values in the northern part of the area follows the regional strike and is associated with shale rather than amphibolite.

Anomalous phosphorus values between 141S and 213S, in the area north of Mount Minza, appear to be associated with one of the beds underlying the hematitic quartz breccia horizon. It may possibly to related to amphibolite, which has been recorded in a diamond-drill hole at Waterhouse No. 2 Prospect (Ruxton, 1961) as containing, in places, 18% apatite. An examination of the other rocks exposed on the surface (banded ironstone, hematitic quartz breccia, tremolitic siltstone, and limestone) failed to reveal any visible phosphate, nor was apatite recognised in significant amounts in thin sections of those rocks. However, veins of apatite occur in hematitic quartz breccia in the Stapleton North area and at the southern extremity of the Gould area, and the possibility of phosphate of sedimentary origin in the anomalous areas is discussed in Chapter 4.

Thirty laterite samples were collected from two exposures in the Mount Minza locality; these are the two occurrences that overlie faults near 189S and south of 213S respectively (Plate 3). Copper, lead, cobalt, nickel, and vanadium assays were not anomalous; in three samples phosphorus values to 1500 p.p.m. were recorded. These results indicate that, at least in the area sampled, base-metal enrichment in laterite does not take place.

Profile sampling of the A, B, and C soil horizons was carried out on two traverses wherever the three horizons were intersected and clearly defined. On traverse 213S, some of these samples yielded anomalous values, and the analyses for copper, cobalt, and nickel are presented in profile form over the anomaly area (Plate 10). The high values are clearly defined in the B and C horizons, but are flattened and somewhat smoothed in the A horizon. It is concluded, therefore, that for reconnaissance surveys the geochemistry of the B and C horizons may be evaluated together, but that the A horizon should be treated separately.

Radiometric. A statistical analysis of radiometric results (Plate 11) suggests that values greater than 0.030 mR/hr may be regarded as anomalous. However, radiometric probing of auger holes revealed only two areas of high radioactivity:

(a) one with a value of 0.077 mR/hr at 285S/396E in lateritic rubble (the high values in this hole occurred only in the top 6 or 7 feet, the values falling to 0.024 in clays of the C horizon); and

(b) a 1600-ft-wide zone of values above 0.030 mR/hr on 141S, centred on 380E where the highest value was 0.070 mR/hr. Again, the values did not increase with depth. This area was located as an airborne radiometric anomaly (Wood & McCarthy, 1952) and is known as Waterhouse No. 4 Prospect.

Waterhouse No. 2 Prospect lies between two of the traverses, and will be examined in detail in 1966.

Geophysical survey

An initial reconnaissance survey was made using electromagnetic Slingram apparatus and Harwell type 1368A ratemeters on traverses 2400 feet apart. Two traverses, A and B, were surveyed with an Askania torsion magnetometer to investigate an airborne magnetic anomaly. The results of the reconnaissance survey are summarised in Plates 8 and 9.

Electromagnetic results. The Slingram reconnaissance survey revealed a very strong conductor at about 448E/213S, 462E/237S, and 470E/237S. Thus it was found necessary to cover most of the area between 420E and 480E from 189S to 241S with traverses at closer spacing. In addition, traverses were extended to the west to 380E between 213S and 237S so that the anomalies found by Daly and Tate (1960) in the Waterhouse No. 2 Prospect could be related to those in the 1965 survey area. The results of this detailed work are discussed in Chapter 4 of this Record.

Clearly defined zones of undisturbed Slingram values occupy a large part of the reconnaissance area. Similar zones of little or no disturbance have been found to correspond to Coomalie Dolomite in previous Rum Jungle surveys. However, in the Gould area, auger drilling showed that the Golden Dyke Formation underlies a considerable part of the undisturbed zones. The drilling indicates that the boundary between the undisturbed (western) and disturbed Slingram results (Plates 8 & 9) coincides well with the western boundary of a zone of amphibolite bodies. The electromagnetic disturbance to the east of this boundary in the northern half of the area should not be inferred as being caused only by amphibolite, as much of this area contains Golden Dyke Formation.

In a further attempt to correlate electromagnetic disturbance with the amphibolite, the boundary between a zone of strong real component disturbance and a zone of strong real and imaginary component disturbance has been added to Plates 8 and 9. This is most clearly defined in the northern half of the area (Plate 8). Comparison of the eastern boundary of the amphibolite with this electromagnetic boundary does in fact show good correlation. Thus it seems possible to distinguish between the effects of amphibolite and Golden Dyke Formation rocks on the basis that amphibolite produces a strong imaginary component disturbance (often off-scale negative) as well as a strong real component disturbance.

The reconnaissance survey provides support for some of the structural features mapped by the geological party in 1965. At about 470E between 45S and 69S, the abrupt displacement of the boundary of the undisturbed zone indicates a possible fault, which agrees with the geological mapping (Plates 2 & 8). It is not possible to infer the trend of the faulting from the geophysical results. A second fault through 213S/423E and 237S/400E (Plate 3) appears to be associated with an axis in the Slingram readings (Plate 9). This axis is continuous with the axis of a strong Turam anomaly found by Daly and Tate at the Waterhouse No. 2 Prospect. The anomaly at Waterhouse No. 2 is not due to a fault, but it seems that the fault in question has provided a suitable environment for mineralisation similar to that found in the prospect. The geophysical results give no indication of the direction of throw in this fault, but the position and trend of the Slingram axis are very close to those of the mapped fault.

The electromagnetic results correlate well with the structure in the Mount Minza area, where the south-plunging anticline is shown clearly by the axial trends of the strong electromagnetic anomalies.

Surface radiometric results. The surface radiometric anomalies detected by the reconnaissance survey are shown as shaded areas in Plates 8 and 9. These anomalies have all been previously investigated, with the conclusion that none of them is associated with uranium mineralisation of economic importance.

Magnetic results. A broad magnetic anomaly discovered by an airborne survey (BMR geophysical map No. G71-92A) trends north-east through the centre of the reconnaissance area. The

position of this anomaly on the ground was determined along traverses A and B (Plates 8 & 9). The shading indicates the magnetically disturbed portions or the traverses. The north-east trend of the aeromagnetic anomaly corresponds well with the trend of the amphibolite, suggesting that the anomalies detected on the ground might show a close correspondence with the detailed mapping of the amphibolite. However, it was not possible to map the amphibolite with sufficient accuracy to show that it was the sole cause of the anomalies.

Conclusions

The reconnaissance surveys outlined two anomalous zones: one north and west of Mount Minza, the other surrounding the Waterhouse No. 2 Prospect.

The Mount Minza area shows low-order geochemical and radiometric anomalies associated in part with intense electromagnetic anomalies. The geochemical anomalies extend between traverses 165S and 237S and are situated approximately in the core of a south to southwest plunging anticline.

In the Waterhouse No. 2 area the geochemical anomalies are mainly between traverses 237S and 261S and are associated with moderate radiometric anomalies.

A few radiometric anomalies were detected in other parts of the Gould area but do not persist with depth. This appears to support the conclusions of earlier investigators that these anomalies do not require further investigation.

A geological connection has been established between the Waterhouse No. 2 Prospect, the Mount Minza anomalies and the Area 65 anomalies. It appears that the hematitic quartz breccia horizon and adjacent shales offer the best prospect of mineralisation.

Recommendations

The results suggest that most of the Gould area may be disregarded with respect to future prospecting for base metals and uranium. The area between the Waterhouse No. 2 Prospect and the Mount Minza anomalies should be investigated in detail by geological, geochemical, and geophysical methods. A detailed investigation of the Mount Minza geophysical anomalies was initiated after completion of the reconnaissance survey, but there was insufficient time to cover all the anomalous area. The results of this examination are described in Chapter 4 of this report.

4. DETAILED SURVEY, MOUNT MINZA AREA

Following upon the conclusions and recommendations in the previous chapter, the Mount Minza anomalies discovered on the traverses spaced at 2400 feet were investigated on traverses spaced, for the most part, at 400-ft intervals.

The supplementary traverses were pegged by the geophysical party and were positioned to cover the most intense of the Slingram anomalies. Additional electromagnetic work, using both Slingram and Turam methods, and surface radiometric work was carried out along them, together with surface geological mapping and auger drilling or surface sampling every 200 feet. Traverses 189S, 201S, 213S, and 237S were surveyed with an Askania torsion magnetometer to test the application of the magnetic method in the area.

The aim of the detailed work was to investigate the extent of the geophysical and geochemical anomalies, to provide geological detail, and to establish, if possible, a correlation between the geology and anomalies west of Mount Minza with those at the Waterhouse No. 2 Prospect.

Geology

An unusual succession of sediments is well exposed in the core of a south-plunging anticline west and north-west of Mount Minza. All the rocks are part of the Golden Dyke Formation. The sequence at Mount Minza is correlatable with that at the Waterhouse No. 2 Prospect (see Plate 12) as follows:

Waterhouse No. 2	Mount Minza
Carbonaceous and graphitic shale	Carbonaceous and graphitic shale
Hematitic quartz breccia	Hematitic quartz breccia
Carbonaceous and graphitic shale	Carbonaceous and graphitic shale
Banded ironstone	Banded ironstone
Tremolitic siltstone	Tremolitic siltstone
	Limestone

There is little doubt that the two sequences are equivalent, although the breccias and banded ironstones are much more prominent in the Mount Minza area. North-trending electromagnetic anomaly axes at the Waterhouse No. 2 Prospect pass at their northern ends into a linear NE-trending anomaly, which in turn passes into the strong Mount Minza anomalies. Isolated outcrops of breccia along the trace of the NE-trending anomaly suggest that the breccia sequence may have acted as a fault plane separating the two areas. Ruxton (1961) previously postulated this fault on geophysical evidence.

Ruxton claims that the hematitic quartz breccia at Waterhouse No. 2 fills tension gashes related to this fault. Regional evidence, however, shows that the breccia is probably a sedimentary bed. At Mount Minza, it is intimately related to the banded ironstone, which merges with it when traced northwards; the breccia is recognisable as far north as Area 65. Prominent exposures of breccia immediately west of the railway line on traverse 333S are identical with the Waterhouse No. 2 breccia, and appear to trend into it, although exposures are masked by laterite to the south of Waterhouse No. 2. Tremolitic siltstone is interbedded with the breccia in the exposure on traverse 333S.

The tremolitic siltstone is an unusual rock and has previously been referred to as 'well bedded siltstone' (Wyatt & Alle, 1953; Ruxton, 1961). It consists predominantly of quartz, tremolite, and sphene in fresh specimens; in most exposures, however, the tremolite is weathered to a ferruginous material. Hand specimens range from buff and brown to greenish grey. It was probably a dolomitic siltstone converted to its present composition by low-grade regional metamorphism. The close association of the rock with limestone in the Mount Minza area supports this contention.

Limestone crops out locally on the western limb of the Mount Minza anticline. It is a tough, bluish grey rock invariably iron-stained on the surface. In many cases the entire rock is weathered to this material. The rock consists of calcite with clots of chlorite and accessory sphene. The chlorite probably has altered from tremolite, representing original clayey constituents in the limestone. A few specks of chalcopyrite are present in some samples of limestone. The

banded ironstones consist of alternating thin bands of quartz and hematite. Beds are well defined and are commonly brecciated. The hematitic quartz breccia is pink to white. Hematite occurs as isolated grains interstitially to the quartz.

Carbonaceous and graphitic shale is fairly well exposed, but is generally heavily leached and silicified on the surface. Its distribution has been inferred from examination of auger cuttings in conjunction with surface outcrops and from the trend of electromagnetic anomalies.

The transition from carbonate rocks through breccias to carbonaceous and graphitic shales implies a transition from a shallow to a deep water depositional environment, accompanied by a pH change from alkaline to acid conditions - in other words, a similar transition to that between the Coomalie Dolomite and Golden Dyke Formation, where mineralisation is known to occur.

A section through the Golden Dyke Formation in the area west of Mount Minza shows that the formation here is approximately half as thick as it is four miles north, on traverse 45S (4500-5000 feet compared to 8000-9000 feet). This thinning, together with the evidence of carbonate rocks encourages the idea that the Golden Dyke Formation here was deposited on a rise in the sea floor, which developed after the cessation of Coomalie Dolomite sedimentation.

Structure

The rocks of the Mount Minza area are folded into a south-plunging anticline, the outlines of which are shown by marker horizons such as the banded ironstones, and by the electromagnetic contours. A syncline separates this area from the easterly dipping sequence at Waterhouse No. 2 Prospect.

A number of faults, all of which trend north-easterly, cause small to moderate displacements. The most prominent fault passes just north of the Waterhouse No. 2 Prospect, and coincides with a linear electromagnetic anomaly. It is inferred that the hematitic quartz breccia has acted as a movement surface for this fault, as small outcrops of this material are strung out along the fault trace. The movement can be deduced as north-block-east where the fault cuts the hematitic quartz breccia north of Mount Minza, but this could be modified or reversed on the western side of the main structure if there was a large dip-slip component.

Geochemical results

Contours for copper and cobalt are shown in Plate 13 at factorial multiples of 100 p.p.m. The major anomalies are as follows:

(1) Copper values of 200 p.p.m. occur at 213S/448E and 221S/448E. These values correspond to a surface radiometric anomaly and coincide with a Slingram anomaly in black shale.

(2) Copper values of over 800 p.p.m. occur on the eastern ends of traverses 197S and 201S and correspond to an increase in radioactivity.

(3) A diffuse belt of copper and cobalt values greater than 100 p.p.m. occurs in beds underlying the hematitic quartz breccia horizon in the 'nose' of the main anticline. This belt is too ill-defined to relate to a specific geological horizon, but some of the peaks tend to occur over limestone, in which a few grains of chalcopyrite have been recorded.

There are no electromagnetic anomalies associated with (2) and (3).

Phosphate

It has been suggested above that phosphate anomalies in the Mount Minza area may be caused by apatite in amphibolite, as at the Waterhouse No. 2 Prospect (Ruxton, 1961). An alternative explanation is that of phosphate in the sediments; and, in fact, veins of apatite are exposed in hematitic quartz breccia at Stapleton North and concentrations of phosphate up to 10% have been recorded in a diamond-drill hole there.

Possibly, the sedimentary and tectonic environment in the Mount Minza area, in which the Golden Dyke Formation is thinner than normal and in which some of the sediments are apparently shallow water deposits, may have favoured phosphate accumulation, in a manner similar to that described by Kaulback (1965).

Slingram results

The real and imaginary component contours for this area are shown in Plates 14 and 15. These show unusually strong real component disturbances in the form of narrow, elongated, deep troughs that extend in a north-south direction for about 5000 feet. The associated imaginary component disturbance is unusually weak and displays only vague trends that are generally similar to the trends in the real component.

The ratio of the real to imaginary component response over this whole anomalous zone is very high, being often as high as eight at the centre of an anomaly, where even a ratio of one would be an indication of significant conductivity. This seems to indicate the existence of near-surface bodies of exceptionally high conductivity, but it must be appreciated that the dimensions of the body also influence the ratio.

On most of the traverses, the anomalies appear as two troughs and sometimes three. The separation of these anomalies is generally so small that a partial merging of the troughs is evident. This renders the treatment of an anomaly purely as a single feature (due to only one conducting body) impossible except on traverse 209S, where the more easterly conductor has been faulted out.

Comparison of the Slingram results with the geological mapping shown in Plate 12 indicates that these anomalies follow the trend of an anticline whose axis trends north through 470E. The strong western anomaly closely follows the outcrop of a thin bed of hematitic quartz breccia. The outcrop lies just to the east of the anomaly. The parallel second and third anomalies fall to the east of the breccia outcrop.

On traverse 237S two anomalies were found, which by their relationship to the breccia outcrop are almost certainly caused by the same body intersected on the two limbs of the anticline. As can be seen from the geological map (Plate 12), traverse 237S cuts almost across the 'nose' of the anticline in the quartzite.

The shape of the Slingram anomalies indicates that they are due to near-vertical tabular bodies. The known geology indicates that except for the anomalies that fall east of 470E, the dip of these bodies is to the west, as this is the western limb of the anticline. A detailed discussion of the dimensions of these bodies follows later.

Geological mapping shows that a fault occurs at 454E/205S and 448E/209S. The displacement of real component contours confirms this fault. It can also be seen in Plate 14 that a displacement of the anomalies occurs at about 454E on traverses 221S, 223S, 225S, and 227S. Geological mapping of this area is prevented by a thick layer of laterite, but it seems probable from these geophysical indications that a fault is present under the laterite.

Turam results

Field experience has shown that the anomaly detected by the Turam method over a conducting body increases in magnitude as the separation between the body and the inducing cable increases. Thus a body whose strike was not parallel to the cable would appear to be a stronger conductor in that part of it which was most distant from the cable than in the part which came nearest to the cable. Therefore there can be no quantitative value in contouring Turam results. The only parameters associated with Turam results that can have quantitative significance are the surface position of the centre of an anomaly and its width about that centre. Therefore the Turam results for this survey (Plate 16) are presented as axes of anomalies; the positions of the corresponding inducing cables are also shown. As can be seen, the position of the centre of the anomaly can be considerably influenced by the position of the cable. In some instances the difference in position between the Turam axis for the same body using two different cables on the same side of the body is as much as 125 feet along the traverse. Thus it seems that some reservations must also be made in using the position of the centre of a Turam anomaly for quantitative purposes.

The Turam axes shown in Plate 16 represent strong anomalies except near the ends, which often represent the fading out of the anomaly. The trends of these axes can be seen to correspond well to the trends of the Slingram axes, which are also shown in Plate 16. The main advantage of the Turam method is its greater depth penetration. This is illustrated in the Mount Minza area on traverse 189S. The Slingram anomaly at 444E on this line is weak and the Turam anomaly strong. Thus it seems that the conducting body plunges to greater depth from 193S to 189S, since both anomalies are strong on 193S.

Tabular near-vertical conducting bodies could produce anomalies of the type found in this Turam survey. This is in agreement with the Slingram interpretation of the type of conductor involved, but apart from some depth information this qualitative treatment of the Turam results adds nothing to the Slingram picture. The fault structures inferred from Slingram results are confirmed in the Turam axial trends.

Surface radiometric results

These results are shown in Plate 17 as contours at intervals of 0.001 milliroentgen per hour (mR/hr). Considerable smoothing of the profiles was necessary before contouring could be attempted. The 0.02-mR/hr contour has been emphasised to facilitate recognition of zones of radioactivity of approximately twice background.

It can be seen that zones of radioactivity greater than twice background occur along the trend of the Slingram axes. These zones might well be continuous with one another but for the interference of superficial cover, such as on traverse 213S where black soil covers all outcrop, and from 227S to 217S, where a thick layer of laterite occurs. There is an elongation of these zones of radioactivity along the trend of the Slingram axes and the zones lie just to the west of these axes in nearly all cases except on traverse 237S. This seems to indicate a definite relationship between conductors and the sources of radioactivity in this area.

A further strong correlation between the conductors and the sources of radioactivity occurs along a north-east trend through about 242E/213S. This is the trend of a fault mentioned earlier, which has associated with it a definite Slingram axis; as Plates 14 and 17 show, a zone of high radioactivity is situated just to the east of this fault and parallel to it.

The geological similarities between Waterhouse No. 2 Prospect and the Mount Minza area suggest that the electromagnetic features of these areas are related. It seems therefore that the radiometric effects associated with the electromagnetic anomalies may also be related.

Subsurface radiometric results

As much of the Mount Minza area consists of rocky outcrops and rubble which were not auger drilled, it was necessary to devise some method of relating surface radiometric readings in areas of outcrop to auger-hole readings in soil-covered areas. To do this, it was assumed that a surface reading on outcrop was equivalent to a subsurface reading in residual soil or weathered rock. Profiles of both surface and subsurface radioactivity were drawn along the traverses and anomalous areas were outlined by deriving the 0.020-mR/hr contour from the combined profiles. Slight differences in calibration between surface ratemeters and subsurface probe units were neglected as it was impossible to apply a uniformly satisfactory correction factor.

The radiometric anomalies are shown in Plate 20. This should be compared with Plate 17, which shows surface radiometric contours. It will be seen that the positions of surface and subsurface anomalies agree quite well and that the subsurface data have tended to extend the limits of the surface anomalies beneath areas of soil; consequently the remarks relating to surface radioactivity apply equally well to the subsurface results with the following modifications:

(a) The main anomaly lying to the west of the hematitic quartz breccia between traverses 193S and 225S is longer than the equivalent surface anomaly and corresponds closely to one of the Slingram anomalies. It also corresponds at its southern end to a copper anomaly. Its southern termination at a laterite outcrop agrees with the position of a fault that passes under the laterite and also with the termination of the Slingram anomaly. Its continuation south of the laterite is shown by the surface anomalies grouped around the nose of the anticline between traverses 229S and 241S.

(b) The anomaly extending northwards from traverse 209S in the north-eastern section of the Mount Minza area agrees with the eastern boundary of the amphibolite in which low radioactivity was recorded. An 800-p.p.m. copper anomaly corresponds to it. The tail of this radiometric anomaly swings south-west along the trace of the fault mentioned above.

(c) A spot anomaly at 197S/460E may be significant in that it corresponds with a 400-p.p.m. copper peak.

Subsurface probing has therefore substantiated the claim that electromagnetic and surface radiometric anomalies have a common source and that this source is in carbonaceous and graphitic shale beds that overlie the hematitic quartz breccia horizon.

Magnetic results

The magnetic work done on traverses 189S, 201S, 213S, and 237S was intended to test the applicability of this method to the problems in this area. Some disturbance, which is probably caused by amphibolite, was found in the core of the anticline. The brief survey proved to be insufficient for the purpose of evaluating the applicability of the method and more magnetic work might be useful.

Quantitative interpretation of electromagnetic results

Several of the Slingram profiles obtained in this area show a strong resemblance to profiles derived from model experiments performed in the Darwin Office of the BMR. The best example of this occurred on traverse 237S as shown in Plate 18. The conducting bodies shown are the result of a combination of the interpretation of both Slingram and Turam results.

The features of the bodies that were derived from the Slingram profiles were: direction of dip, width of the top, position of the centre of the top, and a rough estimate of the depth to the top.

These came from the following considerations, which were derived from model experiments and which are illustrated by the model curves 1 and 2 in Plate 18. The application is for a 200-ft coil separation.

1. The down-dip side of the body is indicated by an emphasised real component peak and an emphasised 'low' in the imaginary component on the down-dip side of the anomaly.
2. For a dipping body of any width, the horizontal distance between either of the top edges of the body and the nearest real component peak is about 125 feet.
3. Regardless of the magnitude of the dip, the centre of the top of the body falls within 30 feet of the centre of the real component anomaly for bodies less than 200 feet wide across the top.
4. The depth to the top may be estimated by the sharpness of the anomaly and to some extent by the ratio of the real and imaginary components. (However, this ratio is also a function of width and conductivity).

These four tentative rules are subject to the following limitations: the dimensions quoted all relate to a coil separation of 200 feet; the models tested so far have all represented bodies of very high conductivity; and models of wide, dipping bodies have yet to be tested. The further work which is planned may show a need for amendment of these rules.

Comparison of curves 1 and 2 with the field curve for traverse 237S show that the dip characteristic is shown well by the imaginary component field curve but that mutual interference between the two real component anomalies has obscured the emphasis of the real component peaks.

Three Turam profiles were obtained on traverse 237S. The first profile, Turam A, was found to be slightly inaccurate and was therefore repeated, giving Turam B. The Turam ratio and phase values were used to derive the real and imaginary component curves and these were analysed to obtain the positions of the current comcentrations corresponding to the anomalies. The results of this are shown in Plate 18 for comparison with the Slingram interpretation.

The three Turam profiles of Plate 18 admirably illustrate the effect, mentioned earlier, of anomaly emphasis with increasing distance from the inducing cable. For curves A and B the cable was 800 feet from the western conductor, while in curve C it was 1200 feet away with a corresponding doubling in the anomaly's amplitude. Another feature of interest is the fact that the phase difference anomaly shows a slight displacement to the up-dip side of the ratio anomaly. This effect is also evident in all the other Turam profiles obtained in this area, the magnitude of the displacement being most pronounced in the northern half of the area. The cause of the displacement is probably the dip of the conducting body, but this is not certain.

Assuming that the current concentrations interpreted from the Turam data are good indications of the true positions of the currents, then any model of the conducting body must be arranged to contain these currents. This was of further assistance in constructing the models shown with the Slingram curve in Plate 18.

Auger drilling of the centre of the western anomaly revealed an exceptionally graphitic black shale. It seems safe to assume that this shale is the conducting body, for drilling results at Waterhouse No. 2 Prospect showed that a very similar carbonaceous and graphitic shale was the cause of the anomaly detected there by Daly and Tate (Ruxton, 1961). The intersection of the base of this shale with ground surface is known on traverse 237S and is shown as point P in Plate 18. Therefore it was possible to construct the model shown by using the following controls:

1. All current concentrations must lie within the body.
2. The width of the top is no more than 120 feet.
3. The centre of the top is at 462.2 $\pm$ 0.3E.
4. The projection of the foot wall must pass through P.

This produced a body with a westerly dip of 69°, a horizontal width of 120 feet, and a depth of 40 feet below the surface. The depths L_1 and L_2 shown in Plate 18 are the extremes of depth to the top of the body permitted by moving the centre $\pm$ 0.3E. L_2 seems to be ruled out by the Turam current points, whereas L_1 places the top too far to the east relative to the real component peaks for a dipping body as shown by the model curves.

The model of the eastern body takes its depth from the western body, its width from the Slingram peaks, and its dip from an attempt to keep the bed thickness as nearly as possible the same as that of the western body. However, the thickness of the bed appears far greater than that of the western body. This is explained by the fact that the western body strikes almost perpendicularly to the traverse, but the eastern one strikes at about 60° to the traverse as can be seen in Plate 14.

An unusual feature of the Turam results occurred on traverses 189S to 201S at about 450E to 454E. The Slingram results indicate the presence of a conductor, yet for the two inducing cables laid to the west, the Turam result registered a strong ratio trough instead of a peak at this location. This is illustrated in Plate 19 where the Turam profile for traverse 201S is shown. The relationship of this trough to the phase anomaly indicates that it is an exaggeration of the trough normally found on the up-dip side of a Turam anomaly and that the peak has been almost totally suppressed. The cause of this is obscure.

The profiles obtained with the cable situated to the east of the anomaly were quite normal with a positive ratio anomaly and provided no assistance in explaining the peculiar behaviour of the profiles obtained with the cable to the west.

Conclusions

The conducting bodies in the Mount Minza area appear to be in graphitic black shale. The investigations of the anomalies in the Waterhouse No. 2 area (Ruxton, 1961) revealed that the top of the conducting bodies apparently coincide with the intersection of the black shales and base of the zone of oxidation. The shale in this prospect is probably closely related to the shale in the Mount Minza area so that we might expect the same criteria to apply to the conductors of the Mount Minza area. It is certain that a high content of graphite exists in the shales well above the base of the zone of oxidation. It is possible that sulphide mineralisation exists in those shales below the zone of oxidation and that this mineralisation, with the assistance of ionic conduction and the graphites, produces exceptionally strong conductors.

A correlation exists between the conductors and zones of higher radioactivity detected on the surface. Again the analogy of the Waterhouse No. 2 Prospect encourages the idea that the surface radioactivity is caused by uranium mineralisation in the carbonaceous and graphitic shale.

There is in general little correlation between geochemical and electromagnetic anomalies; such a correlation does exist, however, at 448E/213S and 448E/221S, rendering the conductor at this locality more promising than elsewhere.

The absence of conductors with the other geochemical anomalies does not, of course, invalidate them, as sulphides could be present here below the limit of detection of the Slingram and Turam equipment.

The conductors are most clearly defined on traverse 237S, but this does not mean that traverse 237S crosses the most likely mineralised environment in the shale. It is not possible to indicate the locality of the highest concentrations of mineralisation in conductors of this kind from electromagnetic data alone. The large number of variables make it possible to say only that very strong conductors exist in this area and that the position of their nearest approach to the surface can be located within 50 feet. The cause of the conductivity is uncertain but high conductivity is often associated with mineralisation. It must be stressed that the conductors cannot be assumed to be of uniform composition throughout their whole length. In view of the known very limited extent of orebodies in the Rum Jungle area, a conducting zone of this type could be investigated conclusively only by testing it with diamond-drill holes situated about every 400 feet along its whole length.

Lack of time prevented detailed investigation of the anomalies leading north to Area 65 from Mount Minza. However, their geological situation indicates that they are a continuation of the Mount Minza area features. Therefore it seems reasonable to assume that the geophysical and geochemical conclusions for the Mount Minza area can be applied to these continuations as well.

Recommendations

At two localities, other factors combine with the electromagnetic anomalies to suggest possible mineralisation:

(1) 213S to 221S at 448E. Copper and radiometric anomalies approximately coincide with the main conductor.

(2) 237S/462E. Electromagnetic anomalies at the 'nose' of the main anticline coincide with a radiometric anomaly.

The following diamond-drill sites are recommended to test these localities:

Collar	Azimuth	Depression	Depth
221S/445E	Grid E	50°	500 ft
237S/459E	Grid E	50°	500 ft

Geochemical sampling and auger drilling was only commenced during the 1965 survey and should be completed by extending the area of detailed work to cover all the geochemical anomalies found in the reconnaissance survey. Particular attention should be paid to auger drilling at Waterhouse No. 2 Prospect.

If the additional auger drilling is to be continued on a 200-ft x 400-ft grid, coverage of the anomalies would involve approximately 50 miles of traverse surveying and 30,000 feet of auger drilling (holes averaging 20 feet). The limits of the extended area should be as follows:

141S - 189S : 432E - 508E
213S - 237S : 360E - 508E
261S - 309S : 360E - 432E

Particular attention should be paid to investigation of the tremolitic siltstone and hematitic quartz breccia for phosphate. It is suggested that all geochemical samples, at least from the hematitic quartz breccia and underlying beds, be analysed for phosphorus, and that field testing of outcrop for phosphate be carried out. Radiometric anomalies in the breccia-siltstone sequence should be regarded as possible indications of phosphate.

5. REFERENCES

ALLE, A. F. 1953a Preliminary geophysical progress report on Waterhouse Uranium Prospect No. 3, NT. Bur. Min. Resour. Aust. Rec. 1953/112.

ALLE, A. F. 1953b Preliminary geophysical report on Waterhouse Uranium Prospect No. 4, NT. Bur Min. Resour. Aust. Rec. 1953/128.

DALY, J. and TATE, K. H. 1958 Geophysical survey at Waterhouse No. 1 Uranium Prospect, Northern Territory, 1957. Bur. Min. Resour. Aust. Rec. 1958/81.

DALY, J. and TATE, K. H. 1960 Waterhouse Nos. 2, 3, and 4 Uranium Prospects geophysical surveys, NT 1957. Bur Min. Resour. Aust. Rec. 1960/109.

DOUGLAS, A. 1962 Waterhouse No. 1 (Area 65) geophysical survey, Northern Territory 1960. Bur. Min. Resour. Aust. Rec. 1962/44.

KAULBACK, J. A. 1965 An approach to the search for sedimentary phosphate. Bur. Min. Resour. Aust. Rec. 1965/37.

LIVINGSTONE, D. F. 1959 Airborne radiometric survey of the Rum Jungle region, Northern Territory 1957. Bur. Min. Resour. Aust. Rec. 1959/9.

MALONE, E. J. 1958 The Geology of the Darwin - Adelaide River area, NT. Bur. Min. Resour. Aust. Rec. 1958/96.

RHODES, J. M. 1964 The geological relationships of the Rum Jungle Complex. Bur. Min. Resour. Aust. Rec. 1964/89.

ROSENHAIN, P. B. and ALLE, A. F. 1953 Preliminary geological and geophysical report on Waterhouse Uranium Prospect No. 1 Northern Territory. Bur. Min. Resour. Aust. Rec. 1953/104.

RUXTON, B. P. 1961 The testing of electromagnetic amomalies by diamond drilling at Waterhouse No. 2 Uranium Prospect, Northern Territory. Bur. Min. Resour. Aust. Rec. 1961/161.

RUXTON, B. P. and SHIELDS, J. W. 1963 Geochemical and radiometric surveys, Rum Jungle, Northern Territory, 1961. Bur. Min. Resour. Aust. Rec. 1963/49.

WOOD, F. W. and McCARTHY, E. 1952 Preliminary report on scintillometer airborne surveys over the Rum Jungle area and other portions of the Northern Territory. Bur. Min. Resour. Aust. Rec. 1952/79.

WYATT, J. D. and ALLE, A. F. 1953 Preliminary report on Waterhouse Uranium Prospect No. 2. Bur. Min. Resour. Aust. Rec. 1953/105.

APPENDIX 1

Geochemical analyses of samples from the reconnaissance survey

Geochemical analyses of samples from the Gould area reconnaissance traverses are listed by co-ordinate position and sample number. The samples were analysed by optical emission spectrograph at the Australian Mineral Development Laboratories, Adelaide.

Results shown in brackets are from mattock samples taken from outcrop or sub-outcrop. All others are bottom-hole auger samples with depth shown. All results are in p.p.m.

A minus sign in front of a number here means 'less than'.

Sample No.	Co-ordinate Position	Cu	Pb	Co	Ni	V	P	Sample Depth (ft)
124045	21S 296E	40	25	100	120	100	120	15
46	300E	10	4	1	6	15	200	17
47	304E	30	6	4	15	50	150	17
48	308E	30	40	20	50	150	150	17
49	312E	30	5	8	15	12	100	17
50	316E	15	4	7	7	8	-100	17
51	320E	60	50	50	50	300	100	17
52	324E	20	2	30	50	40	100	17
53	328E	40	4	100	80	200	-100	17
54	332E	15	1	8	8	20	-100	17
55	336E	25	6	60	40	25	-100	17
56	340E	5	2	7	4	15	-100	17
57	344E	50	40	40	50	200	120	17
58	348E	400	150	80	120	150	200	17
59	352E	15	1	30	40	25	-100	17
60	356E	20	5	11	15	25	-100	17
61	360E	50	70	100	70	250	100	17
62	364E	40	3	80	60	80	-100	17
63	368E	20	3	12	20	120	-100	17
64	372E	50	7	150	200	250	-100	17
65	376E	60	10	100	150	70	-100	17
66	380E	30	12	60	50	25	120	17
67	384E	50	30	80	120	100	-100	17
68	388E	30	12	20	40	120	-100	17
69	392E	10	-1	6	3	6	-100	17
70	396E	10	1	5	12	7	-100	17
71	400E	15	4	8	15	40	-100	17
72	404E	40	3	60	60	200	-100	23
73	408E	20	2	25	50	150	150	17
74	412E	20	8	150	150	120	120	11
75	416E	20	7	60	60	25	-100	18
76	420E	30	25	7	20	120	250	23
77	424E	80	30	80	60	50	250	17
124078	21S 428E	70	12	8	40	100	200	23

Sample No.	Co-ordinate Position		Cu	Pb	Co	Ni	V	P	Sample Depth (ft)
124079	21S	432E	60	20	20	80	150	200	17
124136		436E	30	50	15	40	250	100	1
124080		440E	30	7	7	25	250	250	17
81		444E	20	70	1	8	300	250	23
82		448E	50	15	7	25	120	300	17
83		452E	100	200	7	30	250	200	17
84		456E	25	2	50	60	100	150	17
85		460E	50	100	80	100	500	120	8
86		464E	20	2	7	12	20	150	23
87		468E	30	50	60	60	300	120	17
88		472E	30	4	10	20	40	150	23
89		476E	70	12	50	70	150	300	17
90		480E	20	6	15	25	150	150	17
91		484E	15	50	12	15	25	150	17
92		488E	20	2	15	10	30	200	23
93		492E	20	15	10	25	120	200	17
94		496E	30	25	6	30	150	200	17
95		800E	40	3	20	15	150	120	17
96		504E	(30)	(60	(1)	(15)	300	300	17
124137		506E	(50)	(40)	(12)	(60)	(200)	(-100)	1
124138	21S	508E	(30)	(30)	(40)	(50)	(150)	(120)	1
124217	45S	300E	12	4	10	10	20	300	8
16		304E	10	5	3	15	20	250	11
15		308E	12	5	12	20	20	200	11
14		312E	30	40	50	60	120	200	17
13		316E	15	12	20	40	30	300	11
12		320E	12	12	6	6	25	400	17
11		324E	25	70	8	15	150	300	17
10		328E	20	60	4	15	20	300	17
09		332E	12	15	-1	3	20	500	11
08		336E	20	700	3	12	200	300	17
07		340E	70	150	60	80	15	150	12
06		344E	20	10	6	12	30	300	15
05		348E	8	20	7	4	30	250	11
04		352E	12	150	4	15	120	250	17
03		356E	10	30	-1	3	25	250	11
02		360E	12	200	-1	2	180	300	17
01		364E	30	5	5	25	100	150	11
124200		368E	12	6	6	10	50	120	17
124199		372E	15	7	3	10	150	150	11
98		376E	15	5	3	8	20	200	17
97		380E	20	10	4	6	120	150	10
96		384E	40	3	30	50	25	200	17
95		388E	12	3	40	4	15	120	11
124194	45S	392E	20	8	5	10	100	150	11

Sample No.	Co-ordinate Position		Cu	Pb	Co	Ni	V	P	Sample Depth (ft)
124193	458	396E	20	12	3	25	40	200	17
92		400E	15	8	4	12	40	200	17
91		404E	15	7	6	10	30	150	23
90		408E	12	8	6	7	40	120	17
89		412E	15	10	6	12	70	150	17
88		416E	25	12	8	20	120	200	8
87		420E	25	8	30	50	100	250	17
86		424E	20	7	6	12	100	150	17
85		428E	25	7	4	15	30	150	17
84		432E	15	6	4	25	120	300	17
83		436E	40	12	5	25	150	250	17
82		440E	20	15	4	30	120	150	17
81		444E	20	20	10	30	200	300	17
80		448E	25	3	7	15	25	120	17
79		452E	25	4	20	40	60	120	17
78		456E	30	5	25	25	80	100	17
77		460E	25	2	20	25	30	100	17
76		464E	15	5	8	8	25	120	17
75		468E	100	60	50	100	300	250	17
74		472E	20	15	20	50	120	150	17
73		476E	20	7	25	40	150	100	17
72		480E	20	12	15	10	120	150	17
71		484E	25	3	15	8	150	150	17
124100		488E	15	6	12	6	50	120	17
124099		492E	20	4	15	5	60	150	17
98		496E	30	200	15	60	250	200	17
97		500E	(30)	(50)	(8)	(50)	(200)	(200)	8
124140		502E	(40)	(70)	(10)	(40)	(250)	(-100)	1
124139	458	508E	(40)	(100)	(30)	(50)	(300)	(120)	1
124218	698	300E	4	5	2	6	150	300	17
19		304E	7	3	10	50	20	200	8
20		308E	30	10	40	150	200	250	17
21		312E	10	3	12	15	12	400	14
22		316E	25	12	7	40	150	200	15
23		320E	12	12	10	20	20	250	16
24		324E	15	10	8	15	25	250	11
26		328E	(10)	(2)	(60)	(40)	(10)	(250)	
28		332E	(20)	(15)	(70)	(70)	(50)	(120)	1
27		336E	(12)	(5)	(8)	(20)	(70)	(250)	
25		340E	80	12	200	150	150	500	10
30		344E	20	12	4	20	40	250	11
31		348E	20	70	3	15	30	400	6
32		352E	15	12	5	15	40	150	12
124233	698	356E	12	8	2	7	30	200	11

Sample No.	Co-ordinate Position		Cu	Pb	Co	Ni	V	P	Sample Depth (ft)
124234	69S	360E	20	8	3	6	60	150	11
35		364E	25	8	5	10	120	200	11
36		368E	15	10	3	7	100	200	11
37		372E	12	7	-1	3	20	200	9
38		376E	12	70	1	7	100	400	17
39		380E	15	10	1	4	25	200	11
40		384E	12	8	3	4	20	200	11
41		388E	25	30	12	30	100	120	23
42		392E	70	60	50	50	150	150	17
43		396E	40	12	7	15	100	200	17
44		400E	60	15	6	20	200	250	17
45		404E	50	30	10	15	120	300	11
46		408E	20	15	-1	8	250	250	11
47		412E	40	30	5	10	100	250	11
48		416E	40	50	30	60	150	150	17
49		420E	30	20	8	40	80	150	17
50		424E	70	40	10	40	250	200	17
51		428E	30	8	7	30	300	400	17
52		432E	50	10	50	50	120	500	17
53		436E	40	8	7	60	250	200	17
54		440E	70	7	10	40	500	400	17
55		444E	30	60	5	30	300	500	17
56		448E	20	12	8	15	70	200	1
57		452E	25	50	7	25	250	120	11
58		456E	50	120	10	20	700	150	17
59		460E	25	6	15	25	50	120	11
60		464E	40	70	7	50	250	250	11
124153		466E	(25)	(80)	(7)	(25)	(200)	(-100)	1
54		468E	(20)	(50)	(10)	(20)	(100)	(-100)	1
55		470E	(20)	(58)	(12)	(20)	(200)	(-100)	1
124430		472E	(25)	(12)	(30)	(25)	(25)	(-100)	
124261		476E	12	4	12	3	20	150	11
62		480E	20	5	8	12	70	120	11
		484E 488E	} Not Sampled.						
124152		490E	50	25	30	40	300	200	1
51		492E	80	80	4	25	500	-100	1
50		494E	80	100	4	30	400	120	1
49		496E	40	40	2	20	250	100	1
48		498E	80	60	4	40	300	100	1
47		500E	40	70	5	30	200	150	1
46		502E	60	80	60	150	150	150	1
45		504E	40	50	30	60	200	120	1
44		506E	70	150	3	50	500	-100	1
124143	69S	508E	40	70	3	50	150	150	1

Sample No.	Co-ordinate Position		Cu	Pb	Co	Ni	V	P	Sample Depth (ft)
124327	938	320E	60	4	12	50	50	200	11
26		324E	30	5	70	70	80	250	5
25		328E	12	12	5	100	15	300	13
24		332E	25	20	8	25	60	250	11
23		336E	10	7	-1	12	20	300	20
22		340E	15	12	4	20	180	200	11
21		344E	12	7	2	15	40	300	16
20		348E	25	8	2	30	40	200	14
19		352E	12	8	2	10	30	250	17
18		356E	15	12	7	12	100	200	17
17		360E	20	10	6	12	30	250	23
16		364E	12	8	7	10	25	200	19
15		368E	30	50	10	50	120	200	23
14		372E	150	20	60	120	40	150	23
13		376E	20	25	8	15	70	120	20
12		380E	25	50	12	20	120	150	23
124309		384E	12	6	7	4	15	200	1
10			40	60	40	50	120	150	9
11			12	15	-1	12	150	300	29
124308		388E	15	10	1	15	250	250	17
07		392E	30	20	50	30	150	150	15
06		396E	25	100	4	20	150	200	12
05		400E	20	30	6	10	20	400	1
04			30	70	7	40	200	150	12
03			30	150	15	70	200	200	23
02		404E	40	80	7	20	250	150	13
01		408E	50	100	8	25	150	120	27
00		412E	40	50	15	50	150	150	17
124299		416E	80	15	7	30	300	200	8
98		420E	80	10	5	20	250	250	12
96		424E	25	12	30	20	30	250	1
97			25	10	15	30	200	150	17
94		428E	20	10	20	10	25	300	1
95			30	12	10	25	120	150	17
91		432E	50	25	8	15	200	120	1
92			15	15	7	8	60	300	18
93			40	12	7	12	250	400	23
89		436E	30	5	20	12	70	250	1
90			70	12	20	25	250	300	5
87		440E	25	15	30	40	120	250	1
88			20	15	8	40	120	150	17
86		444E	20	12	10	8	70	200	1
85			30	80	12	30	250	120	15
124284	938	444E	120	30	8	30	200	150	29

Sample No.	Co-ordinate Position		Cu	Pb	Co	Ni	Y	P	Sample Depth (ft)
124283	93S	448E	30	70	12	40	250	200	1
82			25	20	8	15	20	300	9
81			3	2	15	20	25	150	17
80		452E	50	150	40	40	200	200	1
79			12	50	15	8	150	250	4
78			15	3	20	3	150	120	17
77		456E	20	15	7	20	80	150	1
76			25	30	12	40	120	200	9
75			15	3	10	10	40	100	11
74		460E	20	100	25	40	80	150	1
73			25	20	12	40	70	120	6
72			30	15	30	60	200	120	11
67		464E	30	150	50	40	150	200	1
66			60	400	7	40	100	150	7
65			30	2000	2	12	200	400	11
69		468E	20	120	10	12	40	300	1
68			20	150	7	15	120	150	5
64			25	12	12	25	60	150	11
71		472E	12	40	7	4	25	150	1
70			30	50	70	20	150	120	7
63			20	60	6	4	100	150	11
126520		476E	(40)	(150)	(7)	(20)	(15)	(-100)	1
21		480E	(25)	(6)	(10)	(15)	(10)	(-100)	1
124168		484E	(80)	(100)	(80)	(120)	(250)	(100)	1
67		486E	(80)	(100)	(50)	(120)	(300)	(300)	1
66		488E	(50)	(150)	(7)	(50)	(400)	(-100)	1
65		490E	(60)	(120)	(10)	(80)	(300)	(200)	1
64		492E	(30)	(40)	(3)	(50)	(200)	(120)	1
63		494E	(25)	(60)	(1)	(8)	(250)	(150)	1
62		496E	(12)	(10)	(1)	(7)	(20)	(150)	1
61		498E	(15)	(25)	(8)	(80)	(100)	(120)	1
60		500E	(100)	(7)	(70)	(250)	(25)	(600)	1
59		502E	(25)	(40)	(12)	(40)	(150)	(250)	1
58		504E	(60)	(30)	(30)	(50)	(100)	(100)	1
57		506E	(70)	(70)	(80)	(250)	(250)	(300)	1
124156	93S	508E	(80)	(60)	(40)	(120)	(300)	(120)	1
124328	117S	316E	3	5	2	8	120	250	8
29		320E	8	3	4	30	70	200	17
30		324E	12	12	8	40	20	300	12
31		328E	10	40	6	30	15	400	13
32		332E	20	12	8	25	80	250	11
33		336E	20	30	50	40	50	150	11
34		340E	20	12	10	30	150	150	17
35		344E	15	7	8	25	50	200	23
124336	117S	348E	20	12	8	20	40	200	16

Sample No.	Co-ordinate Position		Cu	Pb	Co	Ni	V	P	Sample Depth (ft)
124337	117S	352E	25	40	7	50	120	250	11
124338		356E	15	50	5	20	40	300	11
39		360E	12	40	6	30	30	300	11
40		364E	12	30	6	20	25	250	17
41		368E	20	25	8	15	50	150	17
42		372E	40	70	50	100	40	200	32
43		376E	15	150	2	25	250	400	23
44		380E	30	25	8	30	120	150	17
45		384E	40	40	10	40	200	100	17
46		388E	20	12	7	15	100	100	17
47		392E	25	20	6	20	250	120	17
48		396E	30	50	7	25	500	100	17
49		400E	30	120	2	5	300	250	17
50		404E	100	50	15	120	400	200	13
51		408E	20	10	7	15	120	-100	11
52		412E	30	6	15	30	120	120	17
53		416E	30	5	120	100	200	300	17
54		420E	40	5	50	40	150	-100	17
55		424E	15	2	20	7	40	-100	11
56		428E	15	50	25	10	120	120	11
57		432E	25	2	7	20	120	-100	17
58		436E	20	15	8	20	70	120	5
59		440E	(40)	(30)	(70)	(15)	(150)	(200)	1
60		444E	50	10	20	20	150	100	11
61		448E	20	40	20	10	60	-100	11
124377		452E	(40)	(150)	(50)	(80)	(200)	(100)	1
78		456E	(25)	(150)	(7)	(40)	(80)	(-100)	1
79		460E	(15)	(60)	(3)	(8)	(20)	(150)	1
80		464E	(20)	(20)	(10)	(20)	(40)	(150)	1
81		468E	(25)	(20)	(8)	(25)	(150)	(100)	1
82		472E	(40)	(12)	(8)	(20)	(120)	(-100)	1
83		476E	(20)	(10)	(3)	(7)	(20)	(150)	1
84		480E	(40)	(50)	(2)	(10)	(200)	(200)	1
85		484E	(25)	(7)	(7)	(15)	(20)	(100)	1
86		488E	(20)	(10)	(8)	(25)	(120)	(-100)	1
87		492E	(12)	(15)	(1)	(6)	(15)	(100)	1
124170		494E	(20)	(12)	(3)	(20)	(60)	(100)	1
124169		496E	(80)	(120)	(6)	(120)	(400)	(100)	1
124388			20	20	4	15	120	150	1
124389		500E	(25)	(10)	(8)	(20)	(150)	(200)	1
90		504E	(50)	(12)	(20)	(100)	(150)	(-100)	1
91		508E	(25)	(10)	(12)	(80)	(60)	(-100)	1
125744		512E	(30)	(2)	(15)	(70)	(12)	(-100)	1
45		516E	(25)	(8)	(5)	(12)	(25)	(120)	1
46		520E	(20)	(4)	(1)	(3)	((4)	(-100)	1
125747	117S	524E	(40)	(4)	(15)	(12)	(6)	(120)	1
125748	117S	528E	(30)	(5)	(15)	(12)	(10)	(120)	1

Sample No.	Co-ordinate Position		Cu	Pb	Co	Ni	V	P	Sample Depth (ft)
124541	1418	316E	20	20	6	25	250	-100	10
40		320E	20	7	8	20	40	120	17
39		324E	25	10	10	50	150	-100	17
38		328E	40	30	12	70	200	-100	17
37		332E	20	12	8	30	40	-100	17
36		336E	30	40	20	50	100	-100	14
35		340E	25	15	50	25	80	-100	17
34		344E	70	60	80	120	150	-100	17
33		348E	10	12	40	15	30	-100	17
32		352E	15	8	12	20	30	-100	17
31		356E	25	10	50	80	60	-100	23
30		360E	30	10	5	60	40	-100	17
29		364E	80	780	12	15	20	-100	17
28		368E	20	100	-1	15	400	150	12
27		372E	60	40	2	25	180	-100	12
26		376E	20	4	2	15	30	-100	11
25		380E	404	10	4	25	120	-100	3
24		384E	50	12	5	60	150	-100	11
23		388E	30	20	4	20	150	-100	11
22		392E	25	15	2	15	200	-100	11
21		396E	70	15	5	30	100	-100	11
20		400E	50	30	3	20	120	-100	12
19		404E	20	15	100	40	100	-100	11
18		408E	25	1	50	25	20	-100	17
124517		412E	12	2	12	10	20	-100	11
124375		416E	25	2	30	7	120	-100	17
74		420E	40	60	15	70	200	120	11
73		424E	30	80	12	80	250	200	5
72		428E	12	200	2	4	50	250	5
71		432E	20	60	1	25	100	120	6
70		436E	25	50	7	50	25	-100	14
69		440E	30	50	50	50	30	120	17
68		444E	12	4	4	6	25	-100	17
67		448E	40	3	200	500	20	100	17
66		452E	12	25	15	50	25	120	11
65		456E	25	12	4	60	25	-100	11
64		460E	25	12	8	50	120	-100	11
63		464E	10	3	60	10	12	12004	11
62		468E	7	30	1	5	80	200	6
124392		472E	(50)	(40)	(10)	(20)	(80)	(200)	1
126479		476E	30	40	5	30	100	150	5
124373			(20)	(50)	(20)	(20)	(150)	(100)	1
126480		480E	40	150	6	40	30	150	5
124394	1418	480E	(12)	(15)	(3)	(7)	(10)	(120)	1

Sample No.	Co-ordinate Position		Cu	Pb	Co	Ni	V	P	Sample Depth (ft)
126481	1418	484E	25	100	5	40	25	120	9
124395			(30)	(60)	(8)	(50)	(50)	(120)	1
126482		488E	25	120	10	60	30	120	8
124396			(20)	(20)	(6)	(40)	(15)	(-100)	1
126483		492E	20	40	7	40	20	120	6
124397			(25)	(30)	(10)	(70)	(50)	(-100)	1
126484		396E	20	40	7	40	40	100	11
124398			(30)	(40)	(8)	(50)	(60)	(120)	1
126485		500E	40	50	15	70	75	-100	11
124399			(25)	(10)	(8)	(25)	(40)	(150)	1
126486		504E	25	25	50	70	30	120	8
124400			(25)	(5)	(20)	(100)	(25)	(-100)	1
126487		508E	20	4	10	100	25	150	5
124401			(40)	(6)	(25)	(150)	(150)	(120)	1
125725		512E	(12)	(3)	(2)	(10)	(10)	(100)	1
26		516E	(8)	(2)	(1)	(4)	(4)	(100)	1
27		520E	(25)	(5)	(8)	(10)	(12)	(120)	1
28		524E	(20)	(3)	(8)	(8)	(8)	(150)	1
125729	1418	528E	(20	(3)	(15)	(10)	(4)	(120)	1
124547	1658	316E	10	12	6	30	200	-100	14
46		320E	10	10	7	20	20	200	17
45		324E	12	10	6	30	50	100	17
44		328E	15	20	5	50	70	100	11
43		332E	20	15	5	40	200	-100	15
42		336E	20	12	25	50	50	-100	17
125584		340E	20	12	15	20	50	-100	14
85		344E	10	2	12	50	40	-100	24
86		348E	60	10	40	120	150	-100	17
88		352E	(15)	(2)	(12)	(12)	(120)	(150)	1
87		356E	25	4	3	12	200	100	17
89		360E	(12)	(3)	(3)	(5)	(80)	(150)	1
90		364E	100	70	8	30	200	120	5
91		368E	25	20	3	30	150	-100	11
92		372E	10	10	-1	6	300	120	17
93		376E	40	12	2	25	200	-100	11
94		380E	12	4	4	20	200	-100	16
95		384E	20	12	4	40	200	-100	11
96		388E	70	15	7	30	150	-100	9
97		392E	20	12	4	20	120	-100	5
98		396E	(25)	(10)	(5)	(20)	(50)	(100)	1
99		400E	20	80	2	25	250	150	9
125900		404E	10	10	3	8	40	-100	7
01		408E	25	60	2	20	200	-100	11
02		412E	40	50	50	50	150	-100	13
125903	1658	416E	50	12	6	30	120	150	17

Sample No.	Co-ordinate Position		Cu	Pb	Co	Ni	V	P	Sample Depth (ft)
125904	165S	420E	25	15	7	50	120	120	15
05		424E	10	7	5	10	40	-100	17
06		428E	12	80	7	12	120	120	10
07		432E	25	20	7	15	100	100	17
08		436E	40	5	100	250	100	200	22
09		440E	8	4	2	3	80	-100	23
10		444E	(40)	(5)	(50)	(80)	(10)	(150)	1
11		448E	(30)	(5)	(40)	(40)	(40)	(200)	1
12		452E	7	40	-1	12	300	120	10
13		456E	(25)	(3)	(20)	(30)	(5)	(150)	1
14		460E	30	50	1	12	400	120	10
15		464E	70	30	3	50	400	150	20
16		468E	20	4	70	150	80	600	20
17		472E	30	50	15	80	300	120	20
18		476E	10	20	1	12	250	-100	10
19		480E	150	80	250	800	50	500	10
20		484E	400	300	1200	3000	80	100	10
21		488E	80	60	120	250	300	100	10
22		492E	150	10	400	700	25	700	20
23		496E	200	8	500	1200	20	400	15
24		500E	120	3	300	800	30	100	20
125925		504E	120	3	250	800	20	300	10
124402		508E	6	7	1	4	25	150	1
125739		512E	(10)	(25)	(3)	(7)	(20)	(200)	1
40		516E	(25)	(3)	(8)	(4)	(5)	(120)	1
41		520E	(12)	(3)	(12)	(3)	(7)	(150)	1
42		524E	(25)	(10)	(12)	(7)	(10)	(150)	1
125743	165S	528E	(20)	(5)	(4)	(5)	(7)	(100)	1
125579	189S	316E	8	3	1	10	100	120	11
78		320E	10	4	3	12	200	120	11
77		324E	20	8	5	50	300	100	15
76		328E	20	15	12	40	150	120	11
75		332E	10	3	8	30	100	-100	11
74		336E	12	7	15	70	150	-100	11
73		340E	6	3	7	12	30	-100	17
72		344E	20	15	150	200	50	-100	11
71		348E	20	4	8	100	120	-100	17
70		352E	12	4	70	150	200	200	11
69		356E	30	15	50	50	300	100	11
125568	189S	360E	12	3	25	100	80	150	11

Sample No.	Co-ordinate Position		Cu	Pb	Co	Ni	V	P	Sample Depth (ft)
125567	189S	364E	100	6	15	120	120	100	11
66		368E	70	7	5	40	120	100	15
65		372E	30	20	10	40	250	150	17
64		376E	40	40	8	80	250	120	17
63		380E	20	12	10	40	200	120	17
62		384E	50	50	40	150	500	150	14
61		388E	30	10	3	15	200	-100	17
60		392E	15	6	6	20	250	100	17
59		396E	50	-1	120	600	100	120	11
58		400E	40	1	50	250	100	120	11
57		404E	20	10	7	30	120	120	11
56		408E	15	15	1	12	50	150	11
55		412E	20	6	8	60	100	-100	11
54		416E	20	5	1	12	250	-100	11
53		420E	20	15	1	10	150	-100	11
52		424E	25	15	2	40	200	120	17
125551		428E	15	12	12	40	80	-100	11
124562		432E	100	2	60	250	150	500	35
61		436E	70	25	12	120	150	100	29
60		440E	40	20	6	80	200	100	11
59		444E	40	15	4	40	300	120	4
58		448E	(25)	(6)	(5)	(50)	(100)	(100)	1
57		452E	(25)	(4)	(50)	(150)	(120)	(1000)	1
56		456E	500	3	400	600	250	1500	13
55		460E	20	4	5	50	120	-100	23
54		464E	25	8	6	40	200	-100	11
53		468E	(60)	(100)	(5)	(120)	(300)	(200)	17
52		472E	(70)	(30)	(15)	(250)	(150)	(120)	11
51		476E	(120)	(70)	(6)	(40)	(300)	(150)	6
50		480E	(100)	(250)	(80)	(500)	(60)	(800)	17
39		484E	(70)	(3)	(40)	(250)	(100)	(1000)	23
38		488E	(40)	(4)	(12)	(40)	(250)	(100)	1
124403		492E	(25)	(4)	(12)	(25)	(40)	(120)	1
04		496E	(20)	(7)	(3)	(30)	(300)	(100)	1
125730		500E	(30)	(15)	(3)	(12)	(12)	(120)	1
31		504E	(12)	(3)	(4)	(2)	(8)	(150)	1
125732	189S	508E	(20)	(3)	(7)	(3)	(6)	(120)	1
125583	213S	320E	50	40	15	150	150	150	13
		324E	Not Sampled.						
82		328E	30	40	15	100	250	200	17
81		332E	25	15	12	70	300	150	13
80		336E	25	12	10	60	250	120	17
124548		340E	50	80	80	150	250	-100	12
124549	213S	344E	70	70	30	150	250	120	12

Sample No.	Co-ordinate Position		Cu	Pb	Co	Ni	V	P	Sample Depth (ft)
124563	213S	348E	30	20	10	40	200	-100	5
64		362E	25	15	5	40	300	100	17
65		356E	40	80	50	200	200	150	17
66		360E	40	70	60	150	250	-100	17
67		364E	30	50	50	100	120	120	15
68		368E	30	2	50	70	120	-100	17
69		372E	80	40	12	150	300	-100	23
70		376E	50	40	10	100	250	200	12
71		380E	80	12	50	250	250	-100	1
72			20	7	4	60	200	120	3
73			50	10	30	150	400	120	11
74		384E	15	6	5	15	20	150	1
75			20	10	4	50	200	-100	5
76			15	7	6	40	80	-100	11
77		388E	50	8	15	50	70	120	1
78			40	5	3	20	15	150	15
79			60	50	120	250	80	-100	23
80		392E	30	12	14	120	250	100	8
81		396.5E	15	5	10	40	7	100	1
82			40	25	20	120	200	-100	6
83			50	40	25	200	200	100	11
84		400E	40	5	40	120	50	-100	1
85			70	60	50	150	250	-100	10
86			15	5	-1	7	70	-100	17
87		404E	40	4	25	150	60	100	1
88			40	15	30	120	150	120	9
89			70	2	50	300	15	1500	17
90		408E	30	12	40	60	120	120	1
91			15	4	3	15	20	-100	17
92		412E	30	10	12	20	70	120	1
93			50	12	5	30	150	-100	18
94		416E	12	2	5	5	10	-100	1
95			50	20	12	60	100	150	17
96		420E	20	4	6	7	15	-100	1
97			80	50	20	40	50	200	14
98			25	6	30	60	30	300	17
99		424E	6	2	2	2	20	100	1
124600			12	8	4	7	70	-100	3
125501			6	10	3	12	80	120	6
02		428E	12	6	3	4	15	150	1
03			10	20	10	15	200	150	8
04		432E	12	5	7	10	15	150	1
05			15	10	12	40	150	150	5
06		436E	30	4	8	20	40	120	1
125507	213S		40	5	7	30	100	200	6

Sample No.	Co-ordinate Position		Cu	Pb	Co	Ni	V	P	Sample Depth (ft)
125508	2138	440E	20	6	4	15	30	100	1
09			25	6	3	12	60	-100	4
10			50	12	7	20	250	200	9
11		444E	50	7	20	15	20	150	1
12			120	12	15	100	200	100	5
13		448E	40	8	50	120	120	100	1
14			40	10	200	200	150	-100	3
15			250	50	400	250	700	200	11
16		452E	25	3	8	30	40	150	1
17			40	8	50	150	250	-100	9
18		456E	20	4	10	60	40	-100	1
19			25	12	12	80	200	100	6
20			30	30	12	120	500	120	11
21		460E	100	3	50	250	150	250	1
22			200	5	250	700	200	200	9
23			200	2	100	500	120	500	13
24		464E	70	5	70	150	200	150	1
25			130	5	200	400	150	150	10
26			40	3	50	200	120	120	17
27		468E	80	12	70	250	100	100	1
28			100	20	80	400	150	100	18
29			150	5	150	400	120	-100	23
30		472E	80	10	100	300	120	-100	1
31			100	15	200	200	250	-100	5
32		476E	80	12	80	300	200	100	1
33			80	15	200	300	150	-100	6
34		480E	50	6	25	200	120	-100	1
35			70	20	70	250	250	-100	6
36		484E	70	15	40	300	200	-100	1
37			60	25	30	300	250	-100	6
125733		488E	(40)	(5)	(40)	(120)	(100)	(10)	1
34		492E	Not Sampled.						
35		496E	(5)	(4)	(1)	(4)	(7)	(150)	1
36		500E	(20)	(4)	(8)	(5)	(8)	(200)	1
37		504E	(25)	(3)	(7)	(4)	(10)	(150)	1
125738	2138	508E	(12)	(3)	(15)	(5)	(12)	(120)	1
125635	2378	336E	5	4	8	8	30	-100	1
34		340E	40	12	12	30	30	-100	11
33		344E	30	15	7	25	70	-100	11
32		348E	25	8	5	10	40	120	10
31		352E	20	12	6	30	30	120	17
30		356E	15	15	7	12	25	120	5
49		360E	50	6	120	200	10	-100	17
125648	2378	364E	25	3	25	40	20	100	17

Sample No.	Co-ordinate Position		Cu	Pb	Co	Ni	V	P	Sample Depth (ft)
125647	2378	368E	50	15	15	60	70	-100	5
46		372E	80	200	30	60	70	120	11
45		376E	100	12	60	100	80	-100	17
44		380E	80	50	150	200	40	-100	11
43		384E	80	40	70	250	20	-100	17
42		388E	120	80	700	300	150	120	5
41		392E	80	40	40	100	30	-100	17
40		396E	70	40	12	50	25	300	10
39		400E	300	2500	500	500	30	-100	17
38		404E	50	-1	250	800	50	150	17
37		408E	200	10	20	40	60	300	6
36		412E	25	10	7	40	50	250	5
35		416E	60	12	8	50	25	-100	7
34		420E	20	15	4	15	100	150	11
33		424E	10	8	3	12	80	100	7
32		428E	70	7	20	50	100	200	9
31		432E	40	5	8	60	50	120	7
30		436E	70	8	8	70	100	120	5
29		440E	30	6	7	10	150	120	11
28		444E	60	20	8	25	10	-100	6
27		448E	40	6	7	12	150	300	5
1256 26		452E	100	25	12	70	30	120	5
124417		456E	925)	(6)	(8)	(10)	(15)	(120)	1
16		460E	(10)	(5)	(4)	(3)	(20)	(150)	1
15		464E	(4)	(1)	(2)	(1)	(12)	(-100)	1
14		468E	(25)	(15)	(4)	(10)	(150)	(-100)	1
13		472E	(5)	(6)	(2)	(4(	(20)	(120)	1
12		476E	(8)	(5)	(3)	(2)	(25)	(150)	1
11		480E	(7)	(3)	(3)	(3)	(15)	(150)	1
10		484E	(12)	(12)	(5)	(7)	(35)	(200)	1
09		488E	(4)	(2)	(1)	(1)	(15)	(120)	1
08		492E	(7)	(6)	(2)	(1)	(20)	(120)	1
07		496E	(10)	(6)	(2)	(2)	(20)	(100)	1
06		500E	(6)	(-1)	(3)	(-1)	(6)	(150)	1
05		504E	(12)	(1)	(2)	(1)	(5)	(200)	1
124376	2378	504E	(25)	(4)	(12)	(12)	(20)	(120)	1
125656	2618	336E	10	6	7	10	120	150	10
57		340E	30	10	10	25	20	-100	15
58		344E	30	15	20	40	40	-100	15
59		348E	25	12	15	40	70	-100	15
60		352E	40	20	30	50	70	-100	15
61		356E	60	12	30	40	60	150	10
62		360E	50	15	50	60	70	100	11
63		364E	60	20	70	100	70	-100	11
125664	2618	368E	80	15	40	100	50	-100	11

Sample No.	Co-ordinate Position		Cu	Pb	Co	Ni	V	P	Sample Depth (ft)
124665	261S	372E	50	12	10	50	50	-100	11
66		376E	100	20	15	150	50	-100	11
67		380E	120	10	400	500	50	-100	16
68		384E	40	6	250	700	120	500	14
69		388E	100	50	700	500	80	-100	6
70		392E	80	1	25	200	10	300	16
71		396E	80	12	50	60	60	100	11
72		400E	50	10	40	150	50	150	11
73		404E	120	15	30	70	40	120	6
74		408E	100	12	40	40	60	200	11
75		412E	70	12	20	30	80	200	6
76		416E	80	12	15	25	70	150	11
125677		420E	100	15	7	25	80	150	11
124476		424E	(30)	(5)	(5)	(5)	(50)	(200)	1
77		428E	(20)	(3)	(1)	(2)	(20)	(200)	1
78		432E	(60)	(3)	(4)	(5)	(15)	(150)	1
79		436E	(12)	(-1)	(5)	(1)	(4)	(120)	1
80		440E	(30)	(3)	(10)	(15)	(20)	(-)	1
81		444E	(20)	(3)	(7)	(10)	(20)	(-)	1
82		448E	(15)	(2)	(8)	(8)	(15)	(200)	1
83		452E	(20)	(5)	(10)	(20)	(40)	(200)	1
84		456E	(25)	(3)	(20)	(12)	(15)	(200)	1
85		460E	(20)	(3)	(10)	(20)	(25)	(250)	1
86		464E	(20)	(3)	(6)	(3)	(25)	(150)	1
87		468E	(25)	(2)	(8(	(10)	(15)	(200)	1
88		472E	(15)	(2)	(8)	(12)	(12)	(150)	1
89		476E	(50)	(4)	(50)	(20)	(20)	(400)	1
90		480E	(40)	(3)	(2)	(3)	(25)	(150)	1
91		484E	(30)	(5)	(25)	(15)	(20)	(200)	1
92		488E	(8)	(5)	(3)	(4)	(30)	(150)	1
93		492E	(12)	(3)	(3)	(3)	(20)	(200)	1
94		496E	(20)	(3)	(2)	(4)	(20)	(150)	1
95		500E	(25)	(3)	(6)	(10)	(20)	(120)	1
96		504E	(20)	(3)	(8)	(12)	(15)	(120)	1
124497	261S	508E	(20)	(4)	(7)	(8)	(25)	(120)	1
125695	285S	344E	15	7	6	30	40	120	5
94		348E	10	5	2	25	15	-100	8
93		352E	12	5	-1	25	50	100	11
92		356E	10	3	1	30	15	-100	11
91		360E	12	10	5	40	80	-100	13
90		364E	50	15	10	50	40	100	11
89		368E	100	250	70	150	50	120	11
125688	285S	372E	20	12	7	20	20	100	10

Sample No.	Co-ordinate Position		Cu	Pb	Co	Ni	V	P	Sample Depth (ft)
125687	285S	376E	30	12	17	25	120	120	10
86		380E	25	10	10	20	150	400	9
85		384E	20	3	2	80	150	200	13
84		388E	80	6	80	100	80	250	17
83		392E	25	5	50	40	100	150	11
82		396E	12	3	3	15	30	-100	15
125681		400E	15	5	5	15	120	-100	10
124445		404E	20	5	8	12	25	100	10
44		408E	25	6	12	10	25	120	11
43		412E	25	5	6	7	20	-100	10
42		416E	(25)	(5)	(7)	(8)	(20)	(120)	1
41		420E	(30)	(6)	(6)	(10)	(15)	(100)	1
40		424E	(40)	(8)	(8)	(12)	(25)	(150)	1
39		428E	(30)	(6)	(4)	(3)	(20)	(150)	1
38		432E	(25)	(10)	(2)	(2)	(25)	(250)	1
37		436E	(8)	(12)	(-1)	(1)	(12)	(120)	1
36		440E	(12)	(8)	(6)	(2)	(15)	(150)	1
35		444E	(4)	(3)	(-1)	(-1)	(7)	(200)	1
34		448E	(15)	(12)	(7)	(7)	(25)	(150)	1
33		452E	(30)	(150)	(4)	(6)	(30)	(150)	1
32		456E	(20)	(4)	(-1)	(-1)	(4)	(100)	1
31		460E	(15)	(12)	(1)	(1)	(12)	(150)	1
29		464E	(12)	(5)	(4)	(3)	(20)	(200)	1
28		468E	(10)	(3)	(1)	(1)	(20)	(150)	1
27		472E	(20)	(15)	(5)	(4)	(25)	(200)	1
26		476E	(5)	(3)	(1)	(1)	(15)	(200)	1
25		480E	(12)	(15)	(7)	(5)	(20)	(200)	1
24		484E	(12)	(6)	(6)	(3)	(15)	(150)	1
23		488E	(30)	(20)	(10)	(8)	(100)	(200)	1
22		492E	(10)	(30)	(5)	(3)	(30)	(200)	1
21		496E	(20)	(20)	(8)	(4)	(50)	(200)	1
20		500E	(8)	(5)	(5)	(1)	(12)	(150)	1
19		504E	(12)	(12)	(7)	(2)	(12)	(120)	1
124418	285S	508E	(10)	(4)	(6)	(2)	(12)	(150)	1
125496	309S	348E	10	3	3	4	20	150	1
97		352E	10	5	2	15	30	-100	11
98	309S	356E	(25)	(10)	(12)	(70)	(20)	(100)	14
	305S	360E	Not Sampled (Swamp).						
99	305S	364E	25	50	10	25	20	-100	11
125700	305S	368E	30	4	80	150	20	150	12
01	309S	372E	20	12	8	80	50	150	3
125702	309S	376E	25	7	25	60	30	120	5

Sample No.	Co-ordinate Position		Cu	Pb	Co	Ni	V	P	Sample Depth (ft)
125703	309S	380E	30	10	8	120	20	-100	5
04		384E	70	30	80	300	100	150	5
05		388E	50	15	150	250	30	120	5
06		392E	(10)	(3)	(4)	(12)	(15)	(150)	1
07		396E	8	5	3	10	20	-100	6
08		400E	12	10	3	12	25	120	6
09		404E	15	5	3	7	7	-100	14
10		408E	40	15	7	50	30	120	6
11		412E	40	150	4	20	15	120	12
12		416E	50	200	3	25	15	200	12
124498		420E	(25)	(6)	(2)	(7)	(25)	(150)	1
99		424E	(7)	(7)	(-1)	(1)	(15)	(150)	1
124500		428E	(15)	(5)	(3)	(3)	(20)	(150)	1
126478		432E	40	4	6	15	20	150	5
77		436E	30	6	2	12	30	100	6
76		440E	60	15	7	25	20	150	5
124501		444E	(30)	(6)	(6)	(10)	(20)	(150)	1
02		448E	(70)	(15)	(5)	(12)	(100)	(200)	1
03		452E	(60)	(7)	(15)	(15)	(60)	(200)	1
04		456E	(40)	(6)	(30)	(40)	(50)	(200)	1
05		460E	(20)	(8)	(10)	(12)	(100)	(200)	1
06		464E	(20)	(7)	(12)	(15)	(60)	(-100)	1
07		468E	(70)	(40)	(25)	(25)	(120)	(150)	1
08		472E	(25)	(30)	(12)	(8)	(100)	(150)	1
09		476E	(15)	(6)	(1)	(4)	(25)	(100)	1
10		480E	(25)	(20)	(1)	(4)	(20)	(-100)	1
11		484E	(20)	(120)	(1)	(3)	(70)	(150)	1
12		488E	(15)	(50)	(4)	(12)	(30)	(120)	1
13		492E	(12)	(80)	(7)	(8)	(30)	(150)	1
14		496E	(10)	(20)	(3)	(12)	(20)	(-100)	1
15		500E	(10)	(10)	(2)	(3)	(20)	(150)	1
124516	309S	504E	(15)	(40)	(2)	(4)	(40)	(120)	1
125724	333S	344E	12	7	5	40	80	-100	7
23		348E	12	6	5	12	60	120	10
22		352E	15	5	3	10	80	200	6
21		356E	20	10	3	12	30	100	4
20		360E	12	5	1	25	40	100	10
19		368E	(20)	(6)	(6)	(70)	(50)	(1000)	3
18		368E	40	20	10	100	25	100	6
17		372E	(15)	(6)	(4)	(15)	(12)	(100)	1
16		376E	(12)	(5)	(3)	(25)	(30)	(100)	1
15		380E	(30)	(8)	(15)	(200)	(250)	(300)	1
125714	333S	384E	(25)	(7)	(50)	(300)	(50)	(700)	1

Sample No.	Co-ordinate Position		Cu	Pb	Co	Ni	V	P	Sample Depth (ft)
125713	333S	388E	(10)	(5)	(8)	(30)	(150)	(700)	1
124475		392E	(7)	(2)	(2)	(2)	(30)	(120)	1
74		396E	(10)	(4)	(1)	(1)	(30)	(200)	1
73		400E	(12)	(5)	(4)	(40)	(15)	(150)	1
124446		404E	(12)	(3)	(4)	(3)	(12)	(250)	1
47		408E	(12)	(2)	(3)	(2)	(10)	(-100)	1
48		412E	(25)	(7)	(5)	(8)	(20)	(120)	1
49		416E	(20)	(8)	(2)	(4)	(20)	(150)	1
50		420E	(5)	(8)	(-1)	(1)	(50)	(200)	1
51		424E	(3)	(4)	(-1)	(1)	(15)	(120)	1
52		428E	(6)	(7)	(-1)	(2)	(20)	(150)	1
53		432E	(10)	(6)	(1)	(2)	(25)	(150)	1
54		436E	(6)	(2)	(-1)	(1)	(12)	(150)	1
55		440E	(8)	(5)	(1)	(6)	(25)	(200)	1
56		444E	(12)	(4)	(1)	(1)	(15)	(-100)	1
57		448E	(20)	(7)	(2)	(2)	(25)	(200)	1
58		452E	(10)	(3)	(1)	(1)	(8)	(120)	1
59		456E	(8)	(3)	(1)	(1)	(15)	(150)	1
60		460E	(10)	(3)	(3)	(1)	(20)	(200)	1
61		464E	(20)	(5)	(7)	(3)	(25)	(150)	1
62		468E	(15)	(4)	(6)	(2)	(30)	(250)	1
63		472E	(15)	(5)	(5)	(1)	(30)	(200)	1
64		476E	(12)	(4)	(1)	(1)	(20)	(150)	1
65		480E	(25)	(12)	(8)	(6)	(30)	(150)	1
66		484E	(25)	(10)	(30)	(12)	(50)	(120)	1
67		488E	(25)	(15)	(8)	(8)	(70)	(200)	1
68		492E	(15)	(30)	(4)	(1)	(20)	(200)	1
69		496E	(12)	(4)	(1)	(1)	(20)	(200)	1
70		500E	(25)	(8)	(10)	(3)	(25)	(200)	1
71		504E	(20)	(5)	(15)	(6)	(12)	(120)	1
124472	333S	508E	(40)	(40)	(25)	(25)	(20)	(120)	1
126467	A*	80E	30	20	10	30	20	-100	6
66		84E	60	50	12	50	80	-100	8
65		88E	80	30	12	40	25	100	11
64		92E	70	40	8	40	30	150	2
63		96E	150	500	6	30	50	150	11
62		100E	50	30	12	40	25	100	11
61		104E	50	3	10	30	10	-100	12
60		108E	40	25	30	40	20	100	8
59		112E	40	100	50	60	200	120	6
58		116E	25	100	1	12	400	150	7
		120E = 165S 416E (Sampled previously).							
126457	A	124E	25	60	40	40	100	120	7

Sample No.	Co-ordinate Position		Cu	Pb	Co	Ni	V	P	Sample Depth (ft)
126450	A*	128E	85	4	20	12	80	3000	17
49		132E	40	40	50	100	30	100	11
48		136E	20	30	8	50	50	100	11
47		140E	30	20	12	60	80	100	17
46		144E	40	20	40	200	40	100	17
126445	A	148E	70	500	50	60	250	600	12
126475	B*	126E	30	50	20	40	120	150	11
		130E = 261S 392E (Sampled previously).							
74		134E	40	7	40	40	20	100	11
73		138E	40	15	8	40	25	100	5
72		142E	30	10	5	30	25	150	8
71		146E	20	5	3	15	25	120	8
70		150E	50	40	15	50	25	150	6
69		154E	70	5	5	15	50	150	12
126468	B	158E	20	5	6	12	25	100	2

* Note: Lines A and B are supplementary traverses trending 143°08'T. with limits as follows:

A0 = 69S, 344E
A210 = 237S, 470E

B10 = 165S, 320E
B160 = 285S, 410E

APPENDIX 2

Geochemical analyses of samples from the Mount Minza area detailed survey

Geochemical analyses of samples from the Mount Minza area are listed by co-ordinate position and sample number. The samples were analysed by atomic absorption spectrophotometer at the Australian Mineral Development Laboratories, Adelaide.

Results in brackets are from mattock samples taken from outcrop or sub-outcrop. All others are bottom-hole auger samples with sample depths shown.

The maximum radioactivity in auger holes is shown in mR/hr.

A minus sign in front of a number here means 'less than'.

Sample No.	Co-ordinate Position		Cu (p.p.m.)	Co (p.p.m.)	Sample Depth	Radioactivity (mR/hr)
125817	189S	420E	14	-6	11	.017
18		424E	62	-6	17	.015
19		428E	45	36	11	.018
20		432E	100	74	35	.013
21		436E	83	24	29	.021
22		440E	74	-6	11	.020
23		444E	45	-6	4	.018
125824	189S	448E	(16)	(-6)	1	-
125835	193S	440E	(14)	(-6)	1	-
34		442E	(10)	(-6)	1	-
33		444E	(8)	(-6)	1	-
32		446E	(8)	(-6)	1	-
31		448E	(8)	(-6)	1	-
30		450E	(10)	(-6)	1	-
29		452E	(20)	(-6)	1	-
28		454E	(130)	(48)	1	-
27		456E	(182)	(65)	1	-
26		458E	(130)	(86)	1	-
125825	193S	460E	(204)	(108)	1	-
125861	197S	420E	46	38	-10	.013
60		422E	87	79	16	.015
59		424E	91	24	5	.013
58		426E	69	33	5	.010
57		428E	72	24	5	.012
56		430E	81	29	5	.016
55		432E	79	19	5	.017
54		434E	58	15	5	.015
53		436E	33	20	5	.024
52		438E	26	14	5	.020
125851	197S	440E	26	10	6	.018

Sample No.	Co-ordinate Position		Cu (p.p.m.)	Co (p.p.m.)	Sample Depth (ft)	Radioactivity mR/Hr
125850	1978	442E	20	11	6	.024
49		444E	(24)	(6)	1	-
48		446E	(10)	(-6)	1	-
47		448E	(10)	(7)	1	-
46		450E	(14)	(-6)	1	-
45		452E	(8)	(-6)	1	-
44		454E	(8)	(-6)	1	-
43		456E	(76)	(7)	1	-
42		458E	(8)	(-6)	1	-
41		460E	403	28	11	.022
40		462E	128	93	15	.014
39		464E	99	49	23	.012
38		466E	113	75	17	.013
37		468E	148	70	11	.014
125836	1978	470E	266	20	11	.012
125862	2018	420E	42	11	5	.013
63		422E	69	18	5	.014
64		424E	68	6	8	.015
65		426E	110	9	5	.016
66		428E	81	9	5	.016
67		430E	69	-6	5	.018
68		432E	42	15	5	.016
69		434E	33	-6	5	.018
70		436E	23	-6	6	.017
71		438E	28	-6	5	.018
72		440E	30	10	5	.015
73		442E	8	-6	5	.017
74		444E	(24)	(6)	1	-
75		446E	(24)	(6)	1	-
76		448E	(16)	(6)	1	-
77		450E	(8)	(7)	1	-
78		452E	(4)	(7)	1	-
79		454E	(14)	(14)	1	-
80		456E	(14)	(16)	1	-
81		458E	(80)	(36)	1	-
82		460E	200	69	6	.013
83		462E	150	56	6	.013
84		464E	165	95	17	.014
85		466E	119	65	17	.015
86		468E	210	103	7	.014
125887	2018	470E	806	235	7	.022

Sample No.	Co-ordinate Position	Cu (p.p.m.)	Co (p.p.m.)	Sample Depth (ft)	Radioactivity mR/hr	
125898	2058 420E	69	15	11	.018	
89	422E	71	11	11	.018	
90	424E	68	6	5	.019	
91	426E	108	10	6	.017	
92	428E	42	-6	4	.021	
93	430E	3	-6	6	.016	
94	432E	3	-6	5	.015	
95	434E	18	6	5	.018	
96	436E	13	-6	5	.017	
97	438E	18	-6	6	.020	
98	440E	5	-6	5	.019	
99	442E	79	6	4	.018	
125900	444E	(104)	(7)	1	-	
01	446E	(100)	(7)	1	-	
02	448E	(16)	(7)	1	-	
03	450E	(10)	(-6)	1	-	
04	452E	(14)	(-6)	1	-	
05	454E	(10)	(11)	1	-	
125906	456E	(158)	(90)	1	.023	
07	458E	200	110	17	.016	
08	460E	224	39	17	.012	
09	462E	172	93	17	.016	
10	464E	495	450	17	.018	
11	466E	95	175	17	.022	
12	468E	219	124	17	.028	
13	470E	114	24	17	.024	
14	472E	782	100	17	.008	
15	474E	328	51	11	.018	
16	476E	148	10	17	.018	
17	478E	40	24	17	.012	
18	480E	131	28	17	?	Readings unreliable
19	482E	110	45	17	?	
20	484E	153	58	17	?	
125921	2058 486E	115	10	17	.010	
125940	2098 420E	79	16	11	.007	
41	422E	99	11	11	.008	
42	424E	70	-6	11	.013	
43	426E	8	9	11	.014	
44	428E	5	6	5	.012	
45	430E	-3	6	5	.021	
46	432E	3	-6	5	.015	
47	434E	5	6	5	.019	
48	436E	3	-6	5	.017	
125949	2098 438E	13	-6	5	.022	

Sample No.	Co-ordinate Location		Cu (p.p.m.)	Co (p.p.m.)	Sample Depth (ft)	Radioactivity mR/Hr
125950	2098	440E	49	6	5	.021
126956		442E	85	-6	5	.025
126941		444E	(55)	(-6)	1	-
42		446E	(70)	(-6)	1	-
43		448E	(26)	(-6)	1	-
44		450E	(14)	(-6)	1	-
45		452E	(8)	(-6)	1	-
46		454E	(14)	(-6)	1	-
47		456E	(16)	(27)	1	-
126314		458E	43	29	5	.012
13		460E	61	69	6	.012
12		462E	296	205	7	.016
11		464E	178	144	8	.010
10		466E	328	135	8	.011
09		468E	143	16	11.2	.022
126133		470E	50	71	11	.019
32		472E	90	95	5	.015
126315		474E	(30)	(26)	1	-
126131		476E	140	60	16	.014
30		478E	110	55	17	.014
29		480E	165	61	9	.014
28		482E	199	45	11	.014
27		484E	70	50	5	.012
126126	2098	486E	55	28	8	.013
125922	2138	420E	115	76	17	.008
23		424E	4	7	6	.010
24		428E	4	-6	8	.020
25		432E	4	-6	5	.022
26		436E	60	-6	6	.023
27		440E	55	-6	9	.017
28		444E	108	11	5	.023
29		448E	305	71	11	.029
30		452E	10	7	9	.016
31		456E	16	11	17	.021
32		460E	240	113	13	.013
33		464E	198	108	17	.015
34		468E	190	129	23	.018
35		472E	264	256	5	.015
36		476E	74	196	6	.017
37		480E	96	115	6	.013
38		484E	33	20	6	.012
125939	2138	488E	(33)	(50)	1	-

Sample No.	Co-ordinate Position		Cu (p.p.m.)	Co (p.p.m.)	Sample Depth (ft)	Radioactivity mR/Hr
126383	2178	416E	140	219	5	.011
82		418E	15	-6	5	.013
81		422E	4	6	4	.020
80		424E	-3	-6	3	.011
79		426E	-3	-6	5	.018
78		428E	-3	-6	5	.019
77		430E	10	-6	5	.017
76		432E	20	6	5	.016
75		434E	13	-6	4	.014
74		436E	119	-6	5	.013
73		438E	91	6	5	.017
72		440E	70	38	5	.015
71		442E	31	40	6	.019
70		444E	38	6	5	.018
69		446E	70	-6	6	.020
126360		448E	(129)	(-6)	1	
126239		448E	50	16	5	.019
126367		450E	(15)	(-6)	1	
126340		450E	16	-6	7	.018
126366		452E	70	-6	5	.012
65		454E	31	-6	5	.015
64		456E	20	11	5	.014
126238		458E	(20)	(-6)	1	-
37		460E	(120)	(96)	1	-
36		462E	(26)	(23)	1	-
35		464E	(35)	(-6)	1	-
34		466E	(86)	(9)	1	-
126324		468E	131	136	6	.011
23		470E	100	178	8	.011
22		472E	85	195	12	.011
21		474E	110	195	5	.012
20		476E	82	113	8	.012
19		478E	80	101	7	.009
18		480E	98	117	7	.009
17		482E	80	33	6	.008
126316	2178	484E	100	50	5	.006
126384	2218	416E	115	29	5	.013
85		418E	64	29	5	.011
86		420E	38	11	5	.018
87		421E	18	-6	5	.018
88		422E	6	-6	5	.013
89		424E	6	-6	5	.016
90		426E	8	-6	5	.020
126391	2218	428E	50	6	5	.016

Sample No.	Co-ordinate Position		Cu (p.p.m.)	Co (p.p.m.)	Sample Depth (ft)	Radioactivity mR/Hr
126392	2218	430E	42	6	5	.015
93		432E	94	9	5	.017
94		434E	70	28	5	.016
95		436E	85	24	5	.013
96		438E	38	44	5	.018
97		440E	34	11	5	.019
98		442E	31	11	11	.017
99		444E	82	14	5	.018
126400		446E	15	-6	5	.016
126401		448E	328	15	5	.020
126226		450E	(60)	(-6)	1	-
27		452E	(10)	(26)	1	-
28		454E	(20)	(80)	1	-
29		456E	(24)	(27)	1	-
30		458E	(40)	(14)	1	-
31		460E	(44)	(23)	1	-
32		462E	(47)	(23)	1	-
33		464E	(90)	(9)	1	-
126325		466E	224	363	10	.016
126351		468E	140	220	5	.011
52		470E	99	76	10	.014
53		472E	85	63	15	.014
54		474E	43	19	17	.015
55		476E	49	24	9	.012
56		478E	46	29	8	.010
57		480E	64	30	8	.010
58		482E	61	76	7	.011
126359	2218	484E	55	46	9	.009
126225	2238	450E	(80)	(-6)	1	-
24		452E	(60)	(7)	1	-
23		454E	(16)	(-6)	1	-
22		456E	(14)	(22)	1	-
21		458E	(10)	(18)	1	-
20		460E	(10)	(12)	1	-
19		462E	(13)	(36)	1	-
126218	2238	464E	(111)	(66)	1	-
126428	2258	382E	68	33	17	.013
27		384E	39	9	11	.015
26		386E	75	20	17	.011
126347		388E	38	15	13	.013
46		390E	61	42	11	.012
45		392E	72	45	17	.012
126344	2258	394E	23	65	17	.012

Sample No.	Co-ordinate Position		Cu (p.p.m.)	Co (p.p.m.)	Sample Depth (ft)	Radioactivity mR/Hr.
126343	2258	396E	8	25	17	.011
42		398E	20	20	17	.013
41		400E	65	35	17	.011
40		402E	68	80	17	.012
39		404E	45	55	17	.012
38		406E	52	101	17	.010
37		408E	475	101	17	.013
36		410E	153	90	17	.007
35		412E	16	20	12	.009
34		414E	4	-6	17	.021
33		416E	20	11	9	.020
32		418E	45	30	17	.020
31		420E	202	61	17	.020
126405		440E	79	20	5	.015
04		442E	70	24	5	.014
03		444E	61	30	5	.016
02		446E	72	29	5	.013
126209		448E	(65)	(23)	1	-
10		450E	(60)	(84)	1	-
11		452E	(26)	(45)	1	-
12		454E	(8)	(-6)	1	-
13		456E	(10)	(-6)	1	-
14		458E	(10)	(-6)	1	-
15		460E	(14)	(-6)	1	-
16		462E	(20)	(-6)	1	-
17		464E	(76)	(23)	1	-
126363		466E	177	52	6	.014
62		468E	(55)	(50)	1	-
61		470E	119	80	7	.010
126360	2258	472E	197	310	5	.009
126208	2278	452E	(104)	(75)	1	-
07		454E	(55)	(20)	1	-
06		456E	(33)	(10)	1	-
05		458E	(20)	(12)	1	-
04		460E	(10)	(-6)	1	-
03		462E	(20)	(-6)	1	-
02		464E	(20)	(17)	1	-
01		466E	(25)	(27)	1	-
126200	2278	468E	(16)	(12)	1	-

Sample No.	Co-ordinate Position		Cu (p.p.m.)	Co (p.p.m.)	Sample Depth (ft)	Radioactivity mR/Hr
126425	2298	382E	39	20	6	.016
24		384E	55	24	5	.015
23		386E	39	24	17	.016
22		388E	27	16	17	.015
21		390E	30	24	11	.016
20		392E	27	-6	11	.016
19		394E	49	469	17	.013
18		396E	173	24	17	.012
17		398E	65	69	5	.012
16		400E	42	24	5	.009
15		402E	79	38	17	.013
14		404E	81	85	23	.012
13		406E	49	38	5	.013
12		408E	27	16	9	.014
11		410E	20	30	5	.010
10		412E	35	20	9	.018
09		414E	42	24	5	.020
08		416E	25	33	11	.016
07		418E	18	-6	5	.013
06		420E	25	9	9	.017
126186		440E	(24)	(-6)	1	-
87		442E	(40)	(17)	1	-
88		444E	(47)	(20)	1	-
89		446E	(33)	(30)	1	-
90		448E	(20)	(10)	1	-
91		450E	(76)	(68)	1	-
92		452E	(40)	(35)	1	-
93		454E	(33)	(22)	1	-
94		456E	(40)	(-6)	1	-
95		458E	(33)	(70)	1	-
96		460E	(8)	(10)	1	-
97		462E	(4)	(-6)	1	-
98		464E	(8)	(-6)	1	-
126199	2298	466E	(14)	(-6)	1	-
126431	2338	382E	31	11	5	.012
32		384E	26	16	7	.016
33		386E	29	6	13	.015
34		388E	100	16	17	.012
126444		390E	41	-6	7	.015
43		392E	29	-6	17	.013
42		394E	42	20	17	.014
41		396E	70	33	17	.014
40		398E	26	15	17	.014
126439	2338	400E	55	48	5	.013

Sample No.	Co-ordinate Position		Cu (p.p.m.)	Co (p.p.m.)	Sample Depth (ft)	Radioactivity mR/Hr
126438	2338	402E	25	20	6	.012
37		404E	31	16	6	.013
36		406E	18	26	11	.017
35		408E	15	-6	11	.017
34		410E	30	-6	7	.015
33		412E	42	-6	6	.014
32		414E	8	-6	6	.014
31		416E	15	6	8	.015
30		418E	8	-6	12	.014
29		420E	10	-6	11	.014
126185		440E	(206)	(-6)	1	-
84		442E	(20)	(-6)	1	-
83		444E	(20)	(-6(	1	-
82		446E	(10)	(-6)	1	-
81		448E	(16)	(-6(	1	-
80		450E	(30)	(-6)	1	-
79		452E	(20)	(-6)	1	-
78		454E	(26)	(-6)	1	-
77		456E	(47)	(-6)	1	-
76		458E	(8)	(-6)	1	-
126519		460.5E	20	6	14	.014
125815		460E	(34)	(8)	1	-
16	2338	462E	(18)	(8)	1	-
125814	2358	456E	(31)	(8)	1	-
13		458E	(14)	(-6)	1	-
12		462E	(14)	(-6)	1	-
125811	2358	464E	(10)	(8)	1	-
125798	2378	440E	64	8	11	.018
99		442E	(19)	(-6)	1	-
125800		444E	32	-6	5	.019
01		446E	(19)	(-6)	1	-
02		448E	52	8	5	.016
03		450E	(16)	(-6)	1	-
04		452E	52	17	5	.014
05		454E	(26)	(20)	1	-
06		456E	(21)	(8)	1	-
07		458E	(11)	(-6)	1	-
08		460E	(7)	(-6(	1	-
09		462E	(42)	(-6)	1	-
125810	2378	464E	(12)	(8)	1	-

Sample No.	Co-ordinate Position		Cu (p.p.m.)	Co (p.p.m.)	Sample Depth (ft)	Radioactivity mR/Hr
125797	241S	450E	(21)	(-6)	1	-
96		452E	(21)	(-6)	1	-
95		454E	(23)	(-6)	1	-
94		456E	(14)	(-6)	1	-
93		458E	(11)	(-6)	1	-
92		460E	(9)	(-6)	1	-
91		462E	(3)	(-6)	1	-
125790	241S	464E	(3)	(-6(	1	-
125786	466E	235S	(5)	(-6)	1	-
87		347S	(5)	(-6)	1	-
88		239S	(3)	(-6)	1	-
125789	466E	241S	(3)	(-6)	1	-
126200	468E	227S	(16)	(12)	1	-
125785		229S	(5)	(-6)	1	-
84		231S	(3)	(-6)	1	-
83		233S	(7)	(-6)	1	-
82		235S	(5)	(-6)	1	-
81		237S	(5)	(-6)	1	-
80		239S	(5)	(7)	1	-
125779	468E	241S	(16)	(13)	1	-
125778	472E	233S	(3)	(-6)	1	-
77		235S	(19)	(-6)	1	-
76		237S	(1)	(-6)	1	-
75		239S	(3)	(-6)	1	-
125774	472E	241S	(5)	(-6)	1	-
125769	476E	233S	(3)	(-6)	1	-
70		235S	(5)	(-6)	1	-
71		237S	(1)	(-6)	1	-
72		239S	(1)	(-6)	1	-
125773	476E	241S	(3)	(-6)	1	-
125768	480E	233S	(7)	(-6)	1	-
67		235S	(7)	(7)	1	-
66		237S	(9)	(-6)	1	-
65		239S	(7)	(-6)	1	-
64		241S	(9)	(-6)	1	-
63		243S	(5)	(-6)	1	-
125762	480E	245S	(5)	(-6)	1	-

Sample No.	Co-ordinate Position		Cu (p.p.m.)	Co (p.p.m.)	Sample Depth (ft)	Radioactivity mR/Hr.
125759	4845	2338	(7)	(8)	1	-
56		2358	(7)	(-6)	1	-
57		2378	(7)	(-6)	1	-
58		2398	(5)	(-6)	1	-
59		2418	(11)	(8)	1	-
60		2438	(7)	(-6)	1	-
125761	4845	2458	(5)	(-6)	1	-
125754	4805	2318	(9)	(-6)	1	-
53		2338	(7)	(-6)	1	-
52		2358	(9)	(-6)	1	-
51		2378	(7)	(-6)	1	-
50		2398	(5)	(-6)	1	-
125749	4805	2418	(7)	(-6)	1	-

PLATE 1

10,000 E
20,000 E
30,000 E
40,000 E
50,000 E
60,000 E

60,000 N
50,000 N
40,000 N
30,000 N
13° 0'
20,000 N
10,000 N
0
10,000 S
20,000 S
30,000 S

To Darwin

North Australia Railway

Rum Jungle Granite

Giant's Reef Fault

Rum Jungle Granite

Woodcutter's

Highway

To Darwin

Stuart

Batchelor

Coomalie Creek

Coomalie Gap West

Finniss River

Gould

WATERHOUSE No. 1

WATERHOUSE No. 4

MT. MINZA

WATERHOUSE No. 2

WATERHOUSE No. 3

Stapleton North

Waterhouse Granite

T.E.P. Mine Grid

Bureau of Mineral Resources, Geology and Geophysics, Darwin 1965

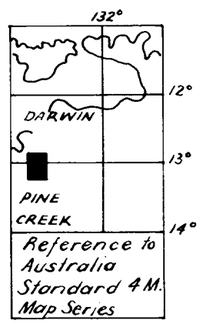

True North

LOCALITY MAP

GEOPHYSICAL AND GEOCHEMICAL SURVEYS

1965

RUM JUNGLE AREA, N.T.

Scale

1 0 1 2 MILES

TO ACCOMPANY RECORD No. 1966/154

D52/B7-193

PLATE 2

GOULD AREA, N.T.

GEOLOGY

Reference

- Formation boundary - full line position accurate, broken line where concealed or approximate
- Lithological boundary - full line position accurate, broken line where concealed or approximate.
- Fault - full line position accurate, broken line position approximate, queried inferred.
- Dip and strike of bedding
- Relative horizontal movement
- —c Costean
- Western limit of auger drilling
- Mallock samples

Lower Proterozoic

Pam Amphibolite

Golden Dyke Formation — **Pld**

- Carbonaceous and graphitic shale
- Quartz hematite breccia
- Banded ironstone breccia
- Limestone
- Tremolitic siltstone
- Siliceous breccia
- Shale, sericitic schist, Undifferentiated

Acacia Gap Tongue — **Pla** Pyritic quartzite

Coomalie Dolomite — **Plo**

- Ferruginous (dolomitic ?) breccia
- Undifferentiated

Crater Formation — **Plr**

- Arkose
- Quartz - tourmaline rocks
- Quartz pebble conglomerate and arkosic grit
- Quartzite
- Quartzite breccia
- Hematitic conglomerate

SCALE 1000 0 1000 2000 FEET

True North

Bureau of Mineral Resources, Geology and Geophysics Darwin, 1965

Sheet 1 of 2 Sheets

TO ACCOMPANY RECORD No. 1966/154

D52/B7-194

PLATE 3

GOULD AREA, N.T.

GEOLOGY

SCALE

1000 0 1000 2000 FEET

Sheet 2 of 2 Sheets

TO ACCOMPANY RECORD No.1966/154

D52/B7-195

Bureau of Mineral Resources Geology and Geophysics, Darwin, 1965

Reference

- Formation boundary - full line position accurate, broken line where concealed or approximate.
- Lithological boundary - full line position accurate, broken line where concealed or approximate.
- Fault - full line position accurate, broken line position approximate, queried position inferred.
- 40 Dip and strike of bedding
- Dip and strike of foliation
- 50 Plunge of small fold axis
- 45 Pitch of lineation on bedding
- c Costean
- Western limit of auger drilling
- Mallock samples

Axis of anticline (plunge indicated)

Axis of syncline (plunge indicated)

Lower Proterozoic

- Pam Amphibolite
- Nolternius Formation — Pln
  - Conglomerate and grit
  - Subgreywacke
  - Siltstone
- Golden Dyke Formation — Pld
  - Carbonaceous and graphitic shale
  - Quartz hematite breccia
  - Banded ironstone breccia
  - Limestone
  - Tremolitic siltstone
  - Siliceous breccia
  - Shale, sericitic schist Undifferentiated
- Coomalie Dolomite — Plo
  - Undifferentiated
- Crater Formation — Plr
  - Arkose
  - Quartz tourmaline rocks
  - Quartzite
  - Quartz breccia
  - Quartz pebble conglomerate and arkosic grit

Laterite

Black Shale

Waterhouse No 2 Prospect

Mt Minza

"Eva Valley"

North Australia Railway

LINE A

LINE B

Scattered laterite

Base Line 180° 00' 00"

143° 08"

True North

165 189 213 237 261 285 309 333

300E 320E 340E 360E 380E 400E 420E 440E 460E 480E

PLATE 4

380E

North Australia Railway

Gould Airstrip

143°08" LINE A

143°08" LINE B

Base Line 180°00'00"

21 45 69 93 117 141 165 189

290E 300E 310E 312E 508E 530E

A10 A30 A50 A90 A110 A130 A150

B10 B40

REFERENCE

Copper	>100 p.p.m.
Lead	>300 p.p.m.
Cobalt	>300 p.p.m.
Nickel	>300 p.p.m.
Vanadium	>250 p.p.m.
Phosphorous	>500 p.p.m.

Western limit of auger drilling

Matteck samples

GOULD AREA, N.T.

GEOCHEMICAL ANOMALIES

True North

SCALE

1000 0 1000 2000 FEET

Bureau of Mineral Resources, Geology and Geophysics, Darwin, 1965

300E 320E 340E 360E 380E 400E 420E 440E 460E 480E

Sheet 1 of 2 Sheets

TO ACCOMPANY RECORD No. 1966/154

D52/B7-196

PLATE 5

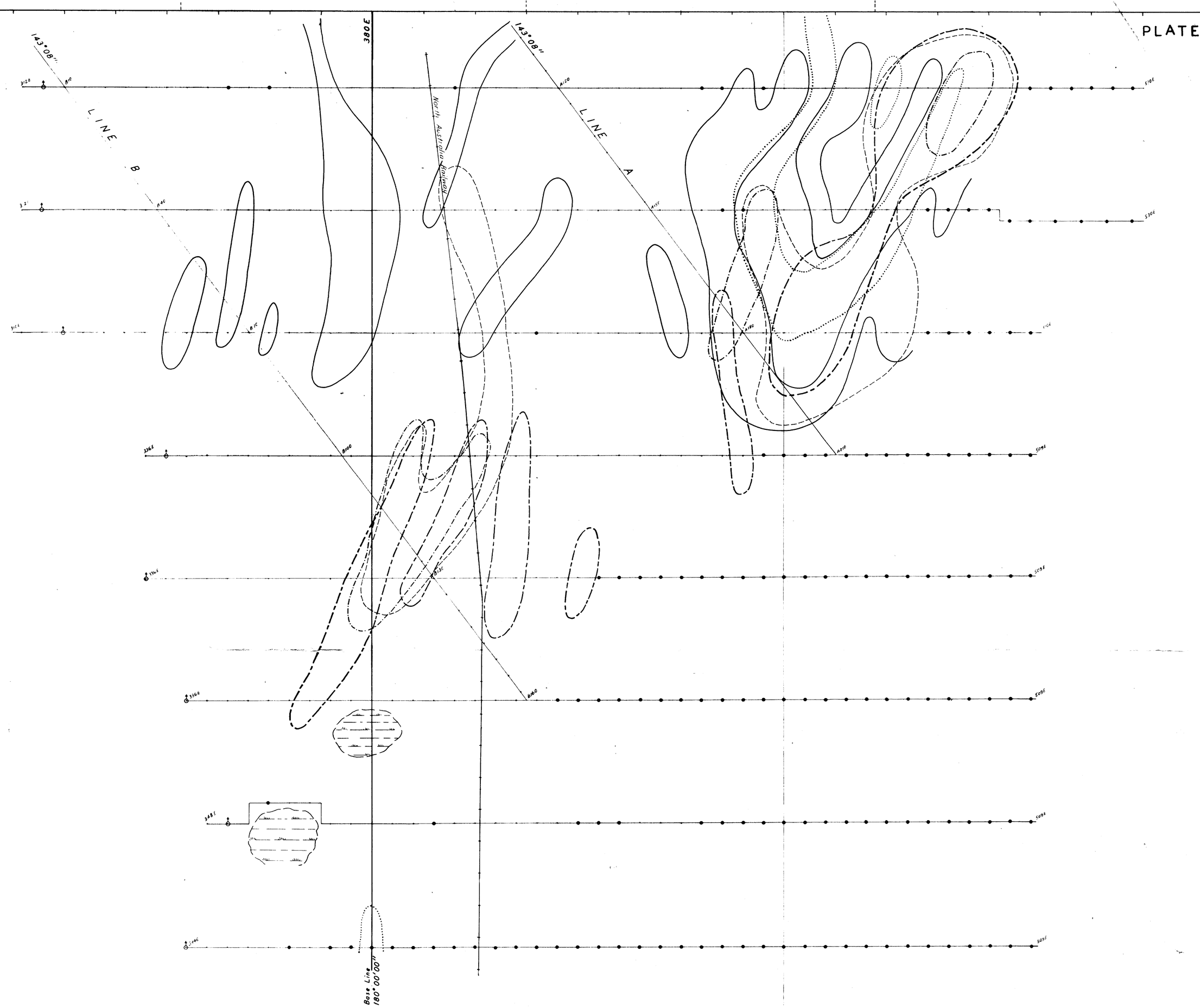

REFERENCE

- Western limit of auger drilling
- Matlock samples
- Copper > 100 p.p.m.
- Lead > 300 p.p.m.
- Cobalt > 300 p.p.m.
- Nickel > 300 p.p.m.
- Vanadium > 250 p.p.m.
- Phosphorous > 500 p.p.m.

GOULD AREA, N.T.

GEOCHEMICAL ANOMALIES

True North

SCALE
1000 0 1000 2000 FEET

Bureau of Mineral Resources, Geology and Geophysics, Darwin 1965

300E 320E 340E 360E 380E 400E 420E 440E 460E 480E

Sheet 2 of 2 Sheets

TO ACCOMPANY RECORD No.1966/154

D52/B7-197

PLATE 6

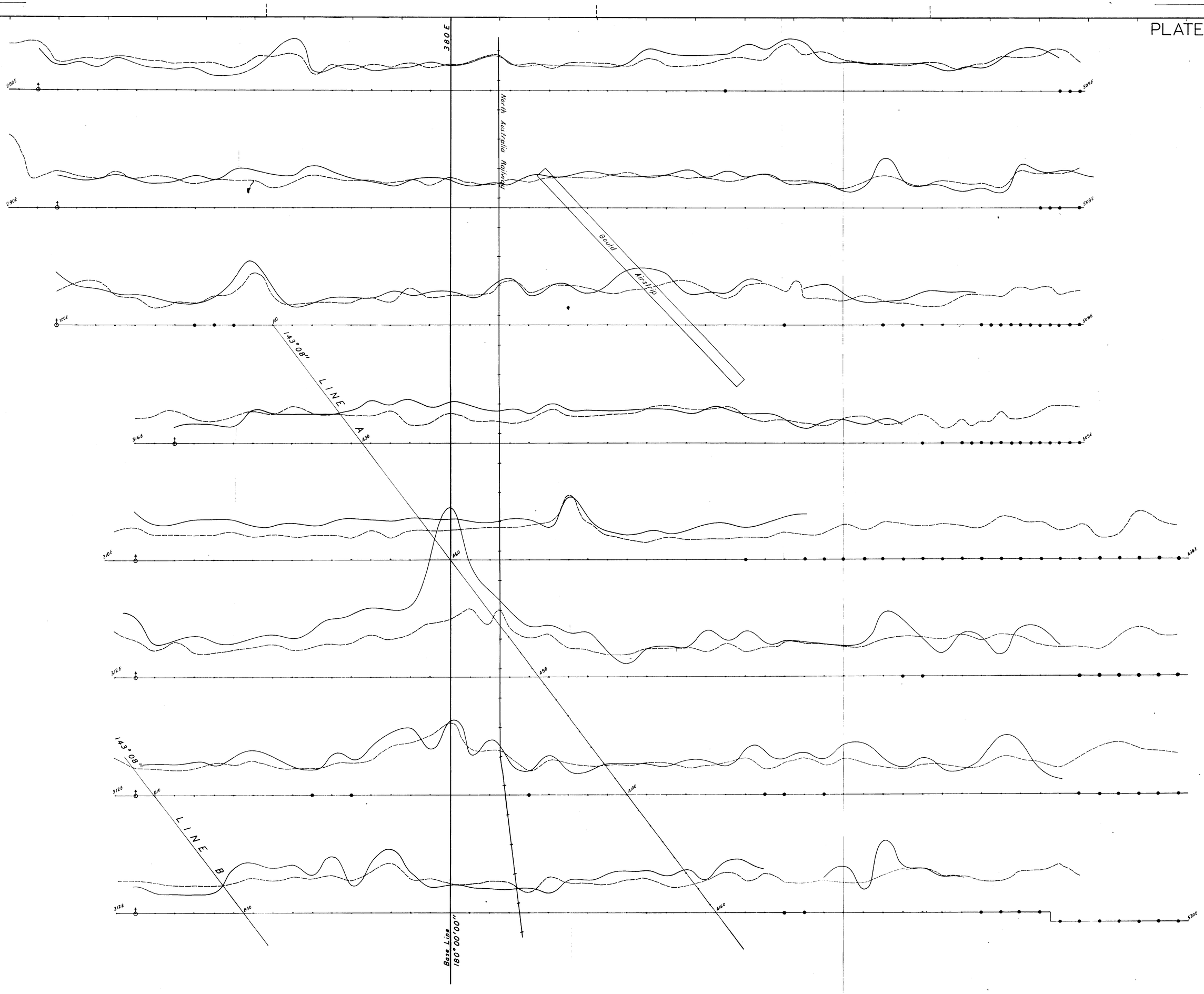

GOULD AREA, N.T.

RADIOMETRIC PROFILES

Western limit of auger drilling

Matlock samples

——— Maximum radioactivity in auger holes (mR/hr)

– – – – Surface radioactivity (mR/hr)

True North

SCALE

1000 0 1000 2000 FEET

Vertical scale: 1" = .020 mR/hr.
(origin on traverse lines)

Bureau of Mineral Resources, Geology and Geophysics, Darwin, 1965

Sheet 1 of 2 Sheets

TO ACCOMPANY RECORD No. 1966/184

D52/B7-198

PLATE 7

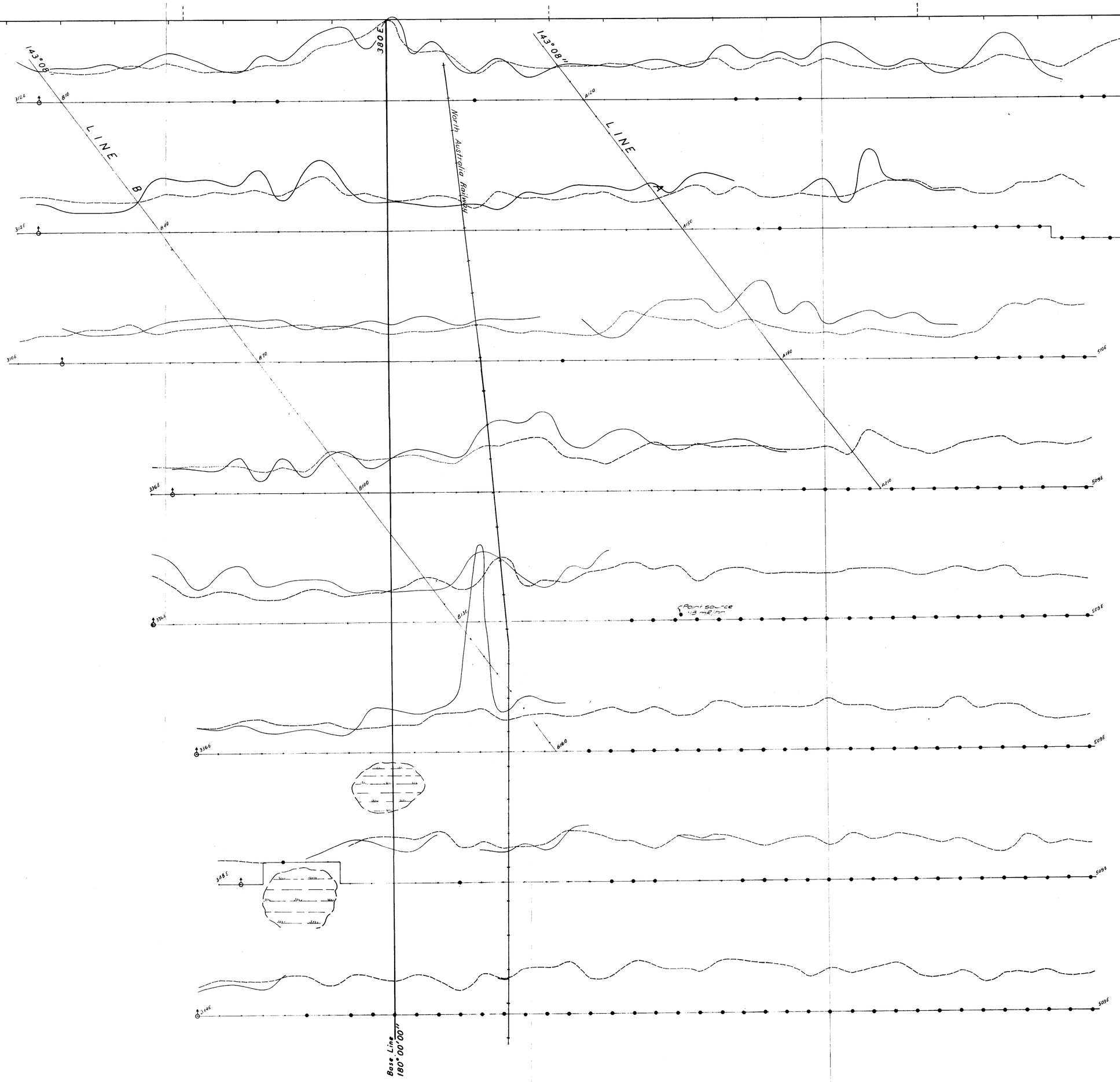

165
189
213
237
261
285
309
333

300E 320E 340E 360E 380E 400E 420E 440E 460E 480E

Western limit of auger drilling

Mallock samples

GOULD AREA, N.T.

RADIOMETRIC PROFILES

—— Maximum radioactivity in auger holes (mR/hr)

– – – Surface radioactivity (mR/hr)

True North

SCALE

1000 0 1000 2000 FEET

Vertical scale: 1" = .020 mR/hr
(origin on traverse lines)

Bureau of Mineral Resources, Geology and Geophysics, Darwin, 1965

Sheet 2 of 2 Sheets

TO ACCOMPANY RECORD No. 1966/154

D52/87-199

PLATE 8

380E

North Australia Railway

Gould Airstrip

Area of strong real component disturbance

Undisturbed

electromagnetic

area

143°08'

LINE A

A30

A60

A90

LINE B

B30

B60

B90

Base Line 180°00'00"

Areas of strong real component disturbance

Area of strong real component disturbance

strong real and imaginary component disturbance

Area of strong real component disturbance

21
45
69
93
117
141
165
189

290E
300E
310E
312E
500E
530E

Accurately defined zones of high surface radioactivity in the Mt. Minza area (Detailed survey)

Electromagnetic boundary

Slingram axis

Zone of high surface radioactivity

Zone of magnetic disturbance

Severe imaginary component disturbance

Severe real component disturbance

Western limit of auger drilling

Matlock samples

GOULD AREA, N.T.

SUMMARY OF GEOPHYSICAL SURVEY RESULTS

SCALE
1000 0 1000 2000 FEET

True North

Bureau of Mineral Resources, Geology and Geophysics, Darwin, 1965

300E 320E 340E 360E 380E 400E 420E 440E 460E 480E

Sheet 1 of 2 Sheets

TO ACCOMPANY RECORD No. 1966/154 D52/B7-200

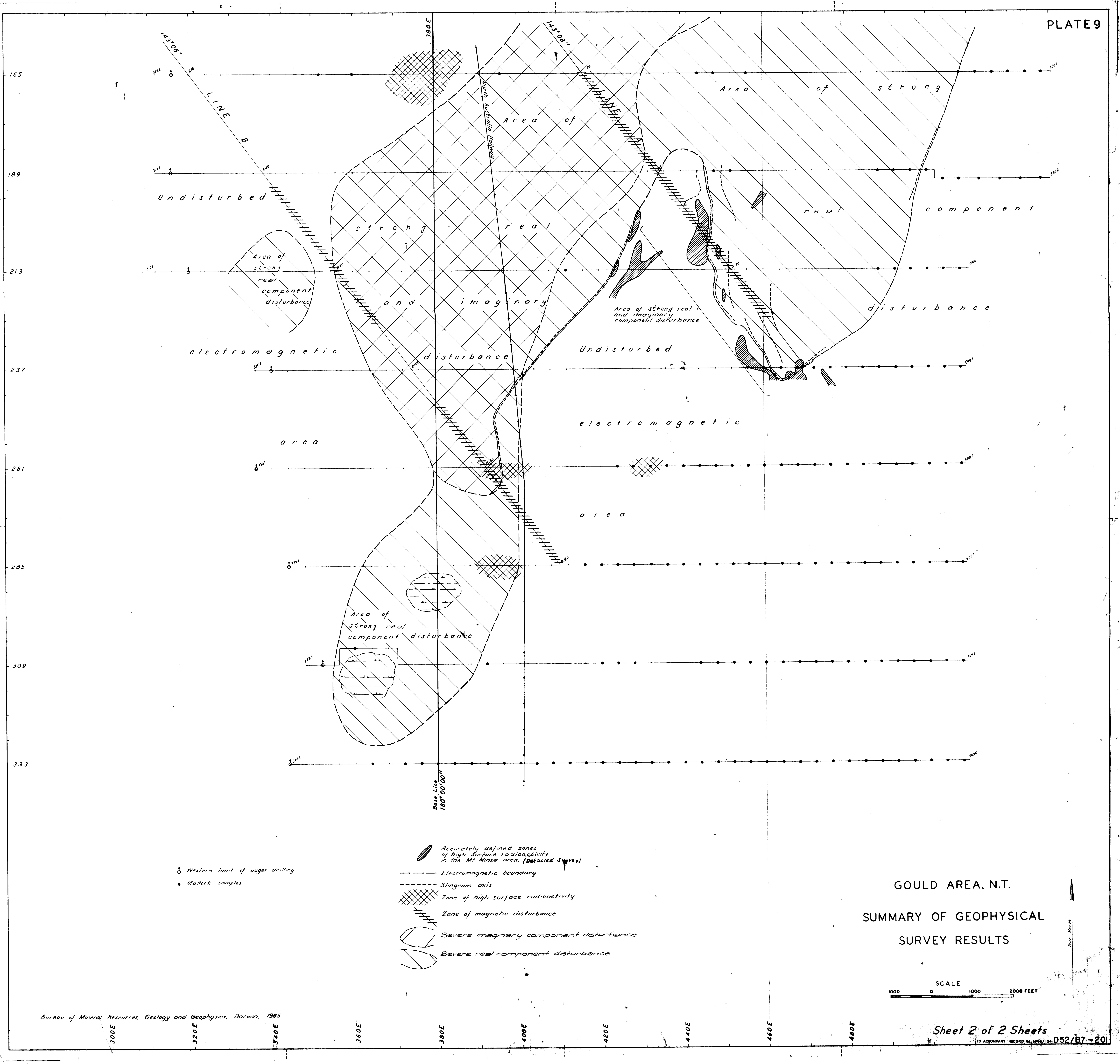
PLATE 9
Area of strong real component
Area of strong real and imaginary electromagnetic disturbance
Undisturbed electromagnetic area
Area of strong real component disturbance
Area of strong real and imaginary component disturbance
real
component
disturbance
North Australia Railway
LINE B
LINE A
143°08''
Base Line 180°00'00''
Area of strong real component disturbance
165
189
213
237
261
285
309
333
300E
320E
340E
360E
380E
400E
420E
440E
460E
480E
Accurately defined zones of high surface radioactivity in the Mt Minza area. (Detailed Survey)
Electromagnetic boundary
Slingram axis
Zone of high surface radioactivity
Zone of magnetic disturbance
Severe imaginary component disturbance
Severe real component disturbance
Western limit of auger drilling
Matlock samples
GOULD AREA, N.T.
SUMMARY OF GEOPHYSICAL SURVEY RESULTS
SCALE
1000 0 1000 2000 FEET
True North
Bureau of Mineral Resources, Geology and Geophysics, Darwin, 1965
Sheet 2 of 2 Sheets
TO ACCOMPANY RECORD No. 1966/104 D52/B7-201

PLATE 10

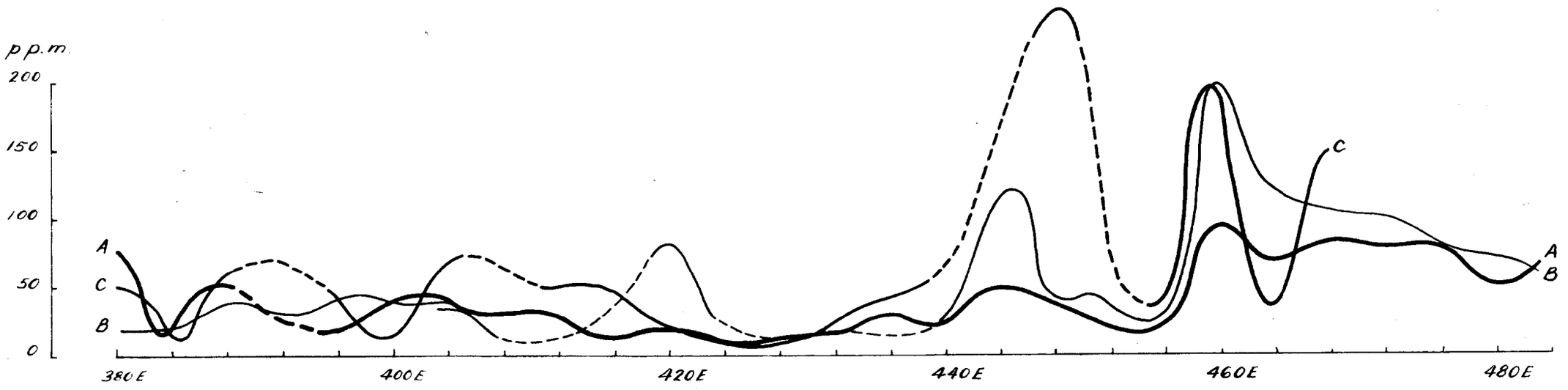

Copper

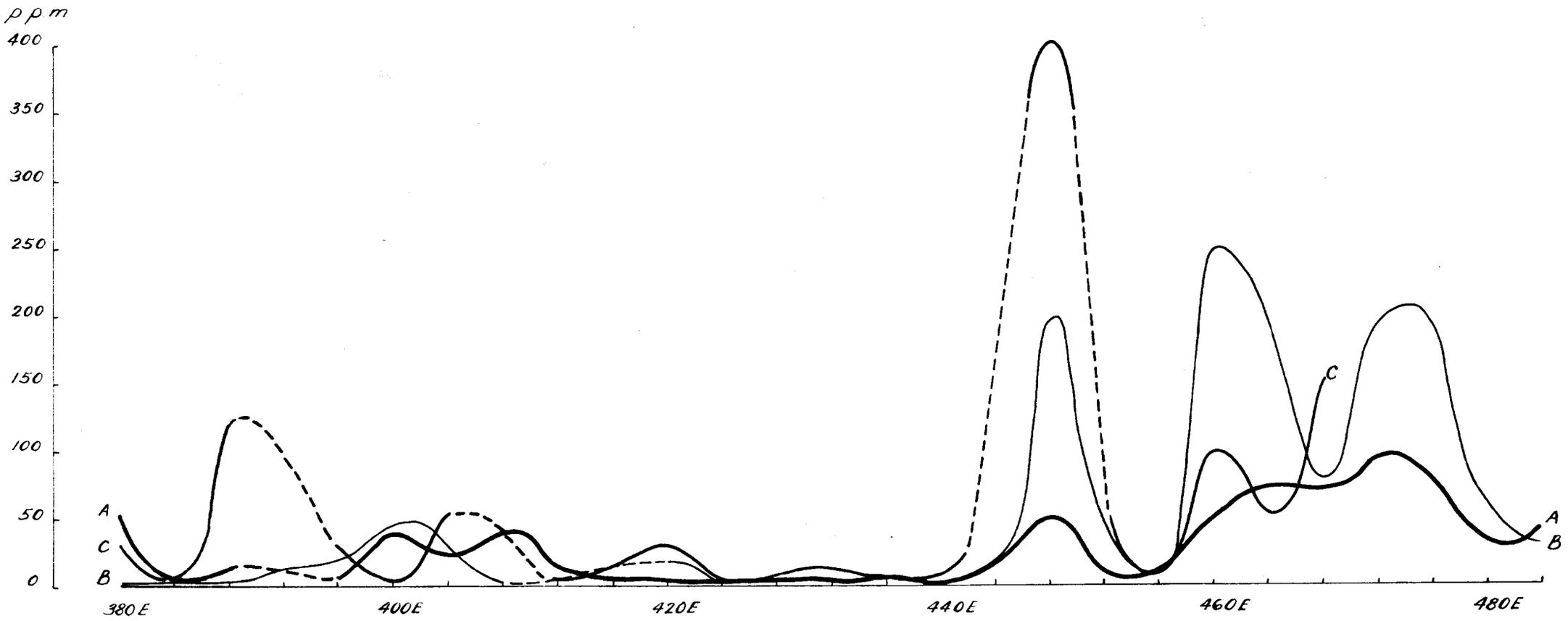

Cobalt

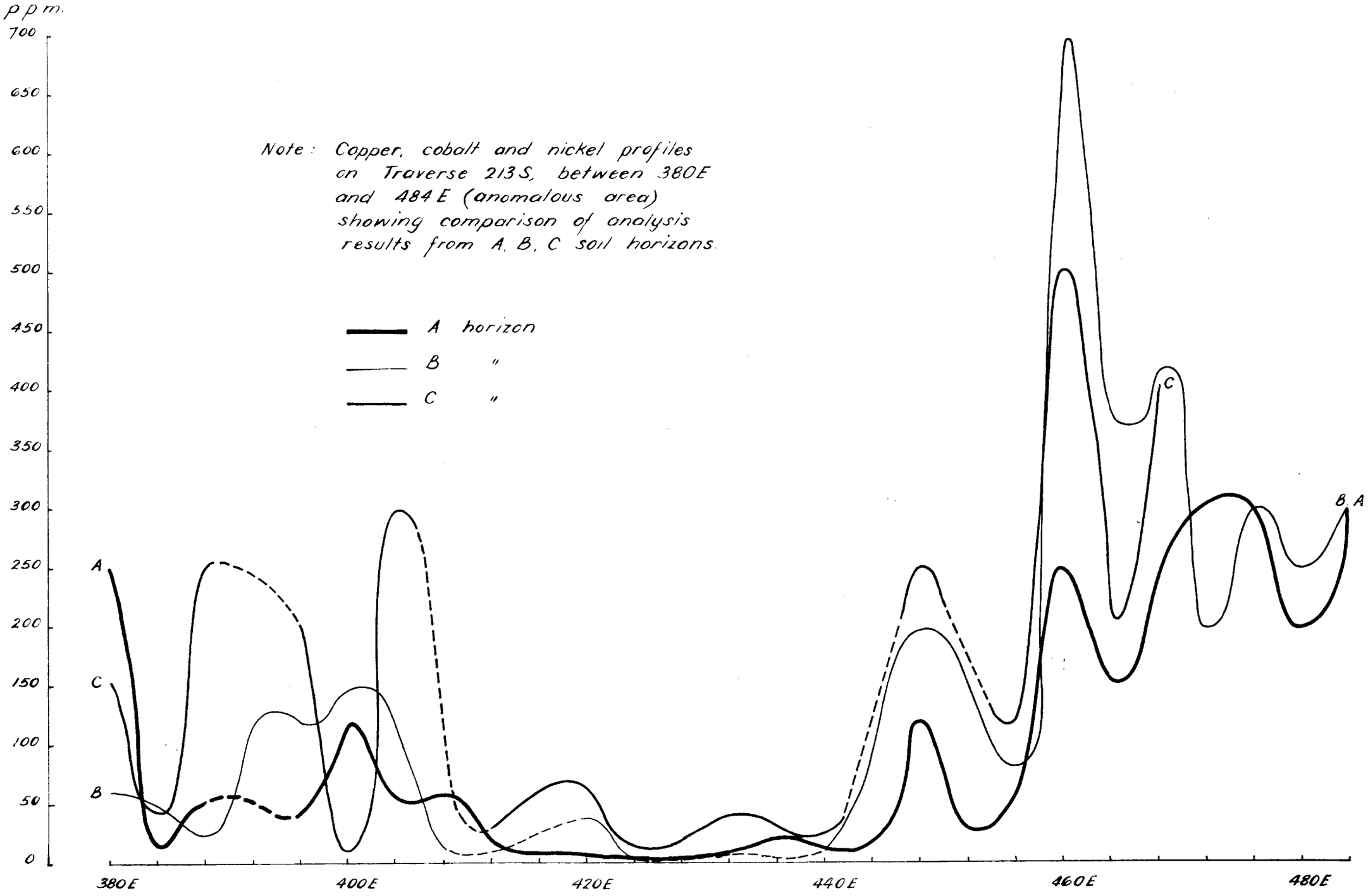

Nickel

Note: Copper, cobalt and nickel profiles on Traverse 213S, between 380E and 484E (anomalous area) showing comparison of analysis results from A, B, C soil horizons.

A horizon

B "

C "

Scale

Horizontal 1000 0 1000 2000 FEET

Vertical 100 0 100 200 P.P.M.

GOULD AREA, N.T.

SELECTED GEOCHEMICAL PROFILES

Bureau of Mineral Resources, Geology and Geophysics, Darwin, 1965

TO ACCOMPANY RECORD No. 1966/154

D52/B7-202

PLATE II

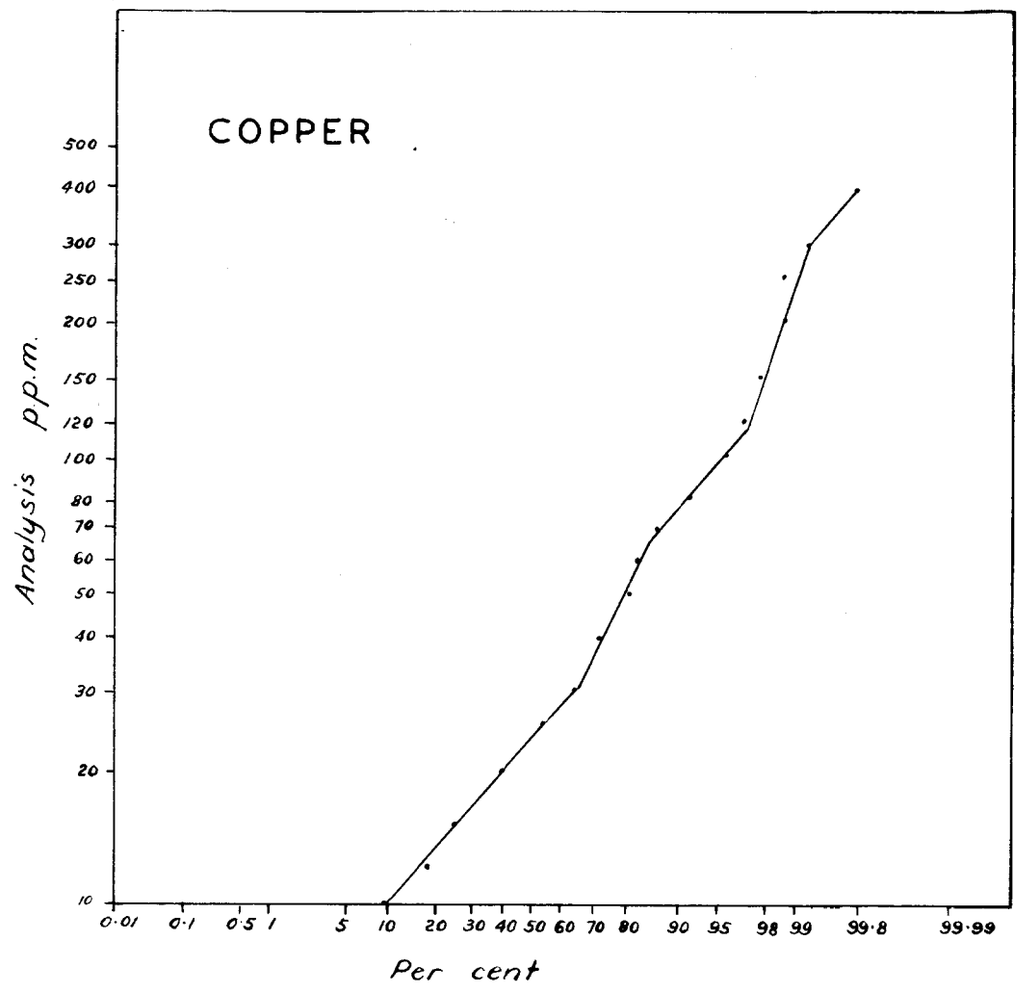

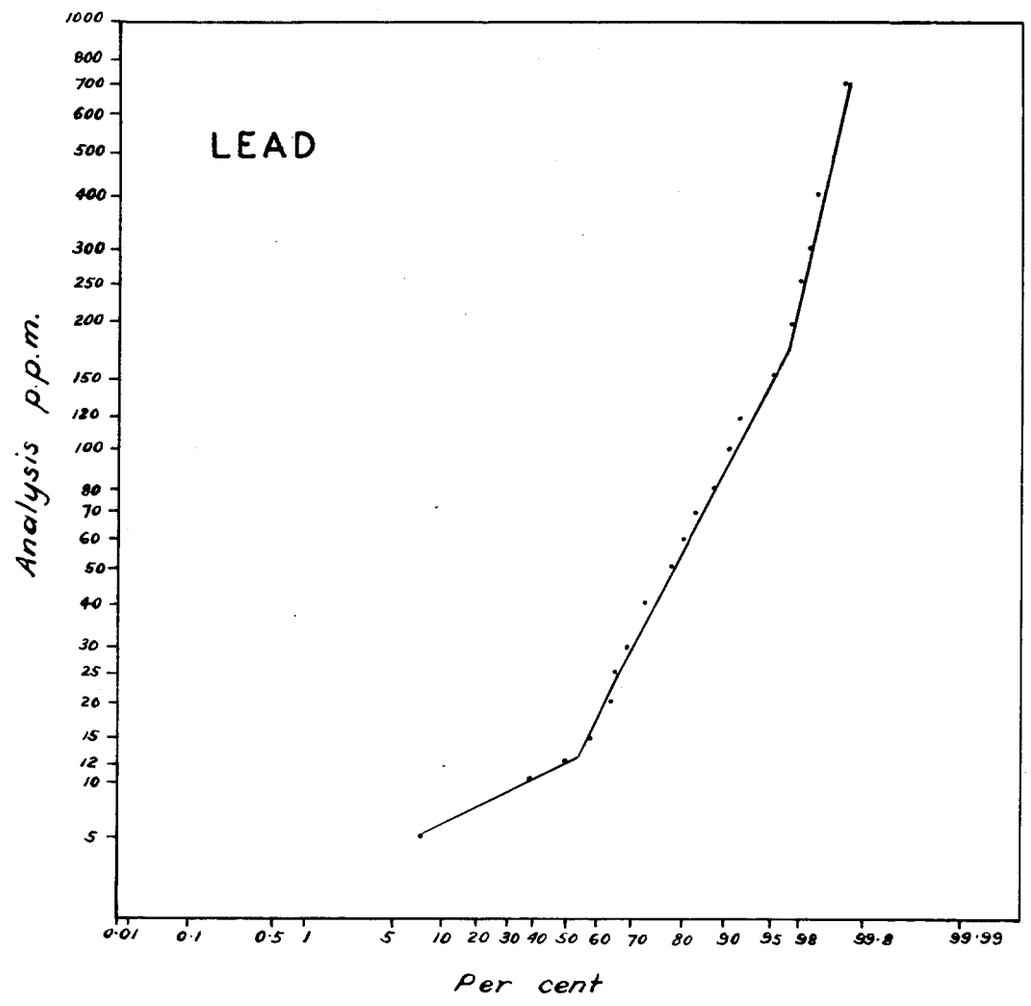

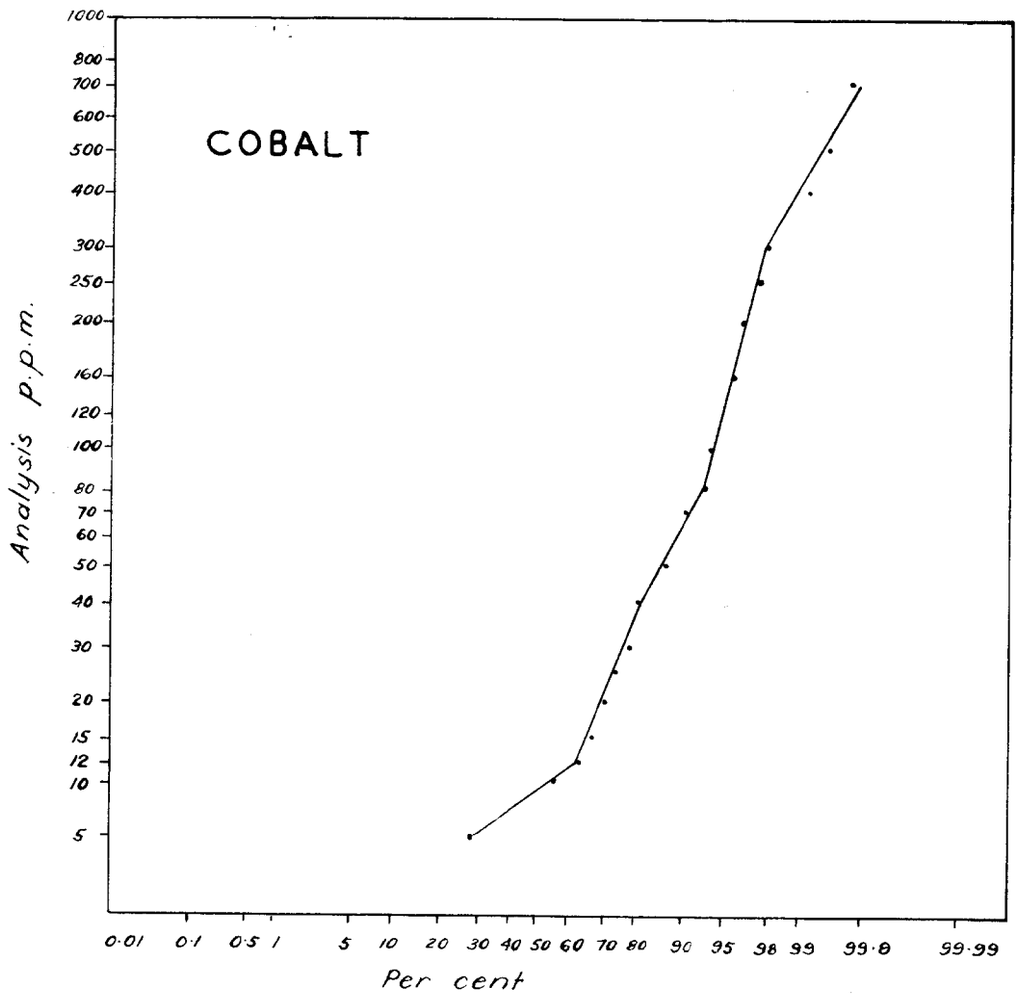

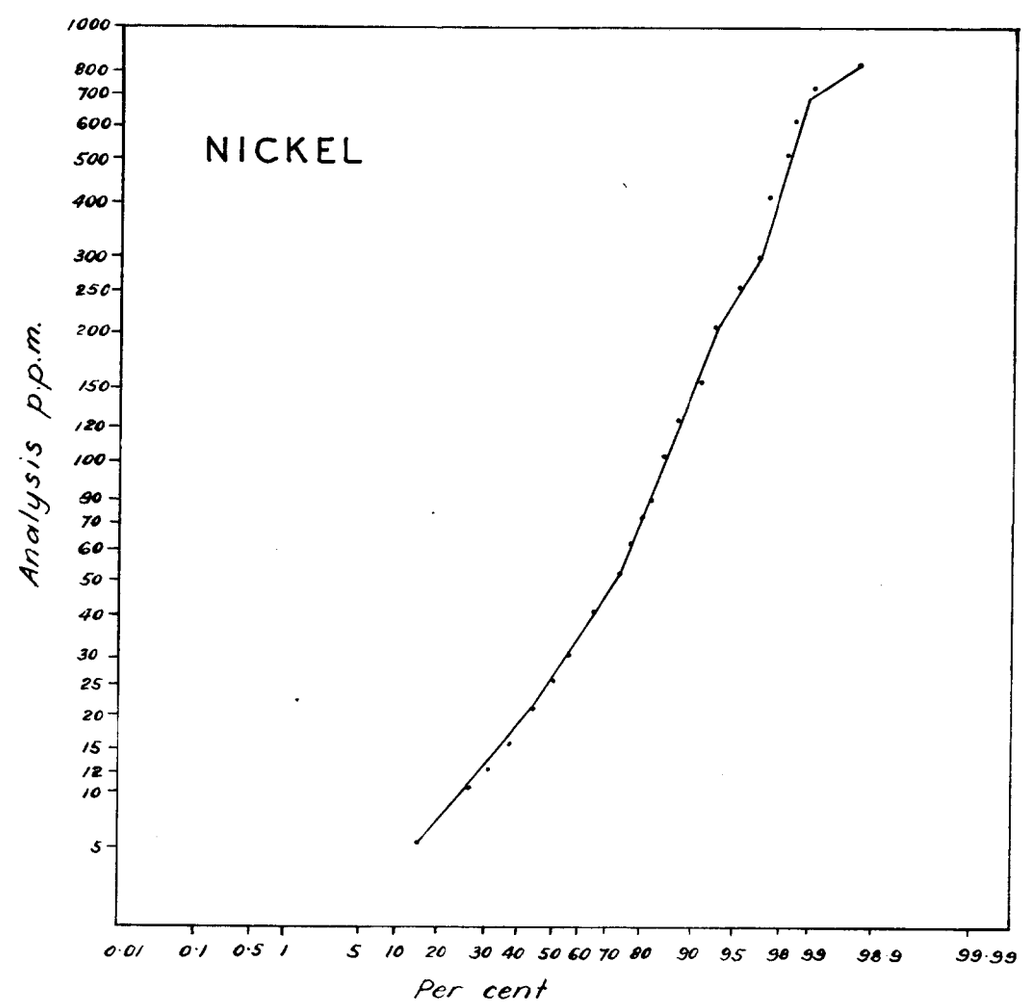

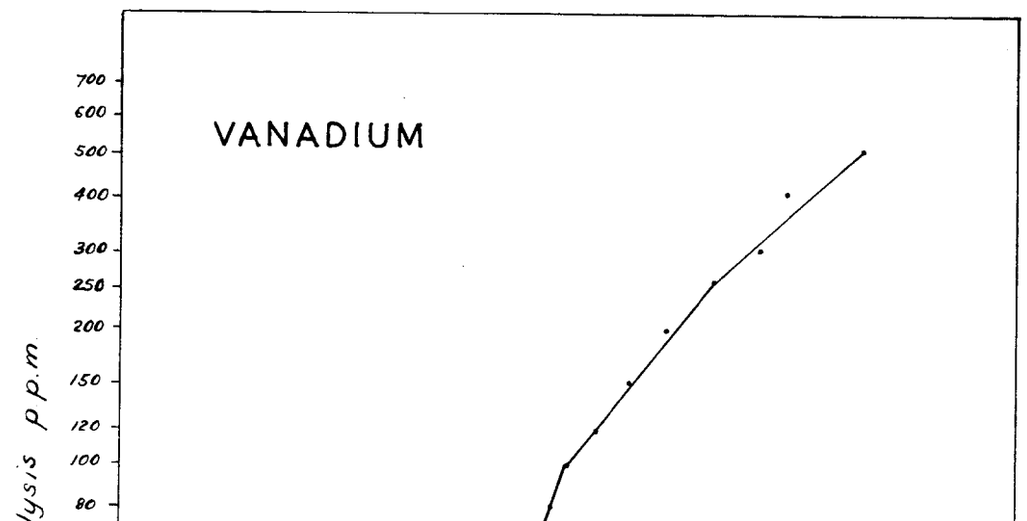

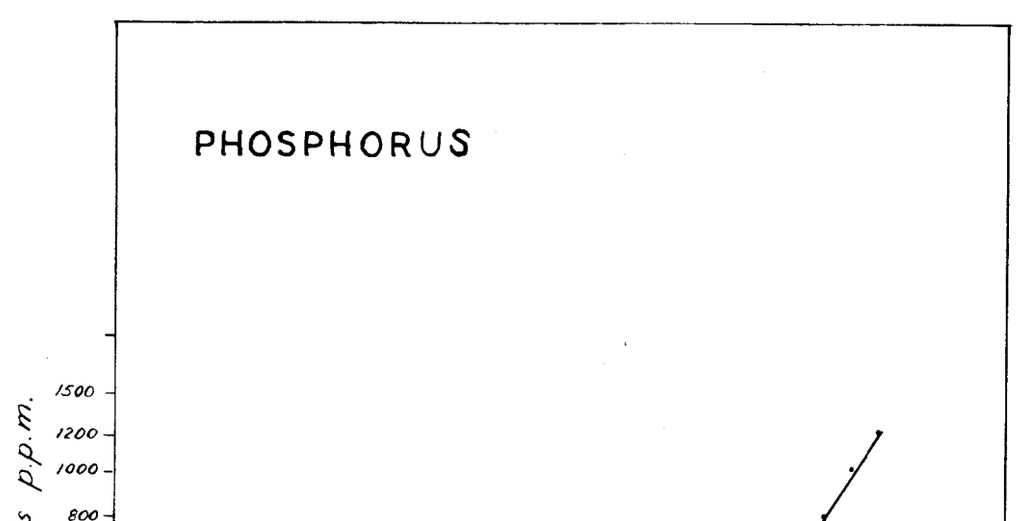

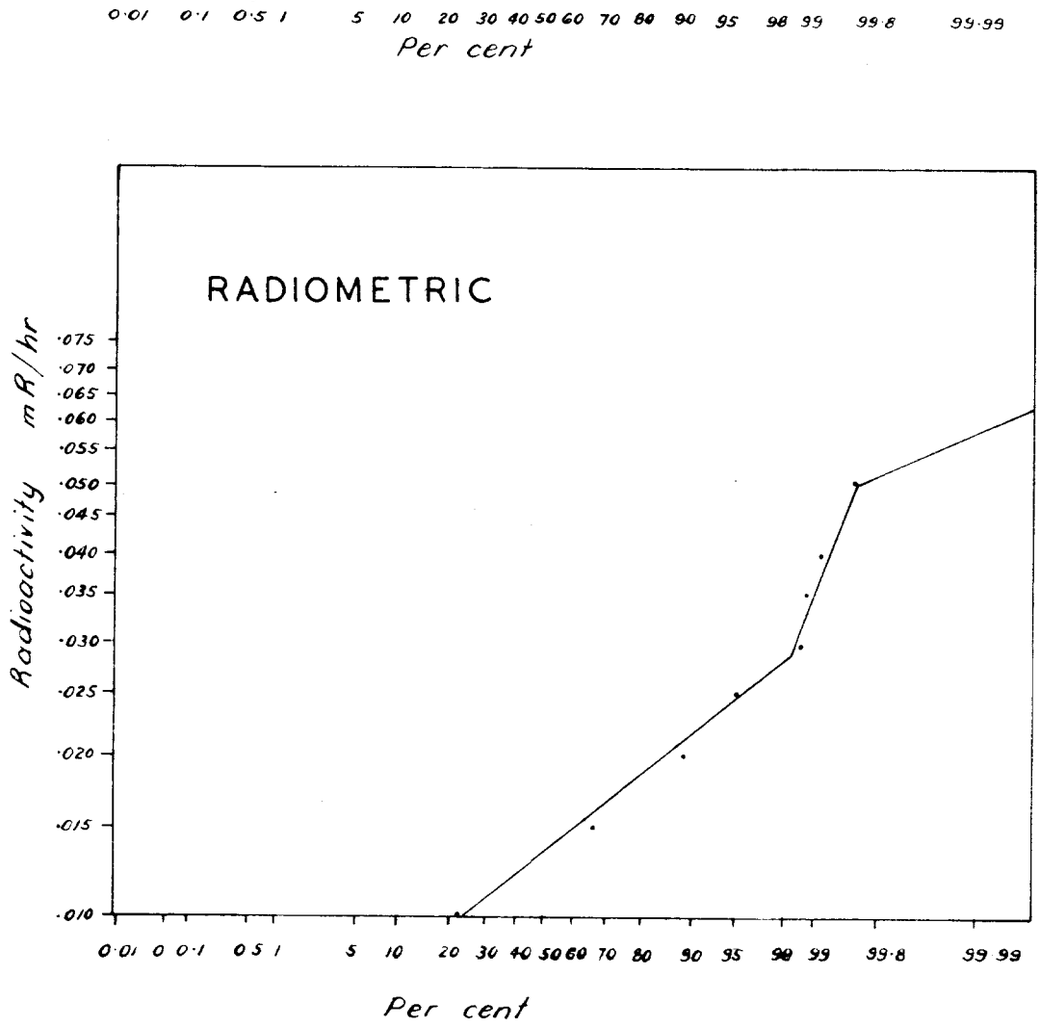

CUMULATIVE FREQUENCY PLOTS OF BASE METAL AND RADIOMETRIC VALUES.

Bureau of Mineral Resources, Geology and Geophysics, Darwin, 1965

TO ACCOMPANY RECORD No. 1966/154 D52/B7-203

PLATE 12

189S
193S
197S
201S
205S
209S
213S
217S
221S
225S
229S
233S
237S
241S
245S

384E
392E
400E
408E
416E
420E
428E
436E
444E
452E
456E
464E
472E
480E
488E

North Australia Railway

Waterhouse No 2 Prospect Grid 1957

Iron post

Iron post

Waterhouse No 2 Prospect

Reference

LOWER PROTEROZOIC
Golden Dyke Formation

- Laterite
- Amphibolite
- Carbonaceous & graphitic shale
- Shale, undifferentiated
- Quartz-hematite breccia
- Brecciated banded ironstone
- Quartzite (silicified shale?)
- Tremolitic siltstone
- Limestone
- Outcrop boundary
- Lithological boundary, concealed or approximate
- Fault position approximate, queried · inferred
- Dip and strike of bedding
- Plunge of minor fold axis
- Costean
- Matlock sample

MT. MINZA - GOULD AREA, N.T.

GEOLOGY

True North

SCALE
400 0 400 800 FEET

Bureau of Mineral Resources, Geology and Geophysics, Darwin 1965

TO ACCOMPANY RECORD No. 1966/154

D52/B7-204

PLATE 13

MT. MINZA - GOULD AREA, N.T.

GEOCHEMICAL CONTOURS

North Australia Railway

Waterhouse No 2 Prospect Grid 1957

iron post

iron post

~100~ COPPER CONTOURS AT 100, 200, 400, 800 P.P.M..

-400- COBALT CONTOURS AT 100 200 400 P.P.M.

NOTE: GEOCHEMICAL CCONTOURS ARE FROM SURFACE AND SUBSURFACE SAMPLES.
SURFACE SAMPLES INDICATED THUS: •

True North

SCALE

400 0 400 800 FEET

189S
193S
197S
201S
205S
209S
213S
217S
221S
225S
229S
233S
237S
241S
245S

384E
392E
400E
408E
416E
420E
428E
436E
444E
452E
456E
464E
472E
480E
488E

Bureau of Mineral Resources, Geology and Geophysics, Darwin 1965

TO ACCOMPANY RECORD No. 1966/154

D52/B7-205

PLATE 14

1895
1935
1975
2015
2055
2095
2135
2175
2215
2255
2295
2335
2375
2415
2455

North Australia Railway

Slingram axis

Iron post

Iron post

Waterhouse No 2

Frequency 1760 c/s
Separation 200 ft.
Contour interval 10%
Peak + Trough I

PLATE 15

1895
1935
1975
2015
2055
2095
2135
2175
2215
2255
2295
2335
2375
2415
2455

North Australia Railway

Iron post

Iron post

Workhorse No 2 Prospect Grid 1957

384E
392E
400E
408E
416E
420E
428E
436E
444E
452E
456E
464E
472E
480E
488E

Frequency 1760 c/s
Separation 200 ft.
Contour interval 10%
Peak + Trough I

MT. MINZA - GOULD AREA, N.T.

SLINGRAM IMAGINARY COMPONENT CONTOURS

True North

SCALE
400 0 400 800 FEET

Bureau of Mineral Resources, Geology and Geophysics, Darwin 1965

D52/B7-207

TO ACCOMPANY RECORD No. 1966/154

PLATE 16

1895
1935
1975
2015
2055
2095
2135
2175
2215
2255
2295
2335
2375
2415
2455

North Australia Railway

Iron post

Iron post

Waterhouse No 2 Prospect Grid 1957

384E
392E
400E
408E
416E
420E
428E
436E
444E
452E
456E
464E
472E
480E
488E

Slingram axis

Turam 440 c/s. showing primary loops and corresponding anomaly axes

MT. MINZA - GOULD AREA, N.T.

TURAM AND SLINGRAM AXES

True North

SCALE

400 0 400 800 FEET

Bureau of Mineral Resources, Geology and Geophysics. Darwin 1965

D52/B7-208

TO ACCOMPANY RECORD No. 1966/154

PLATE 17

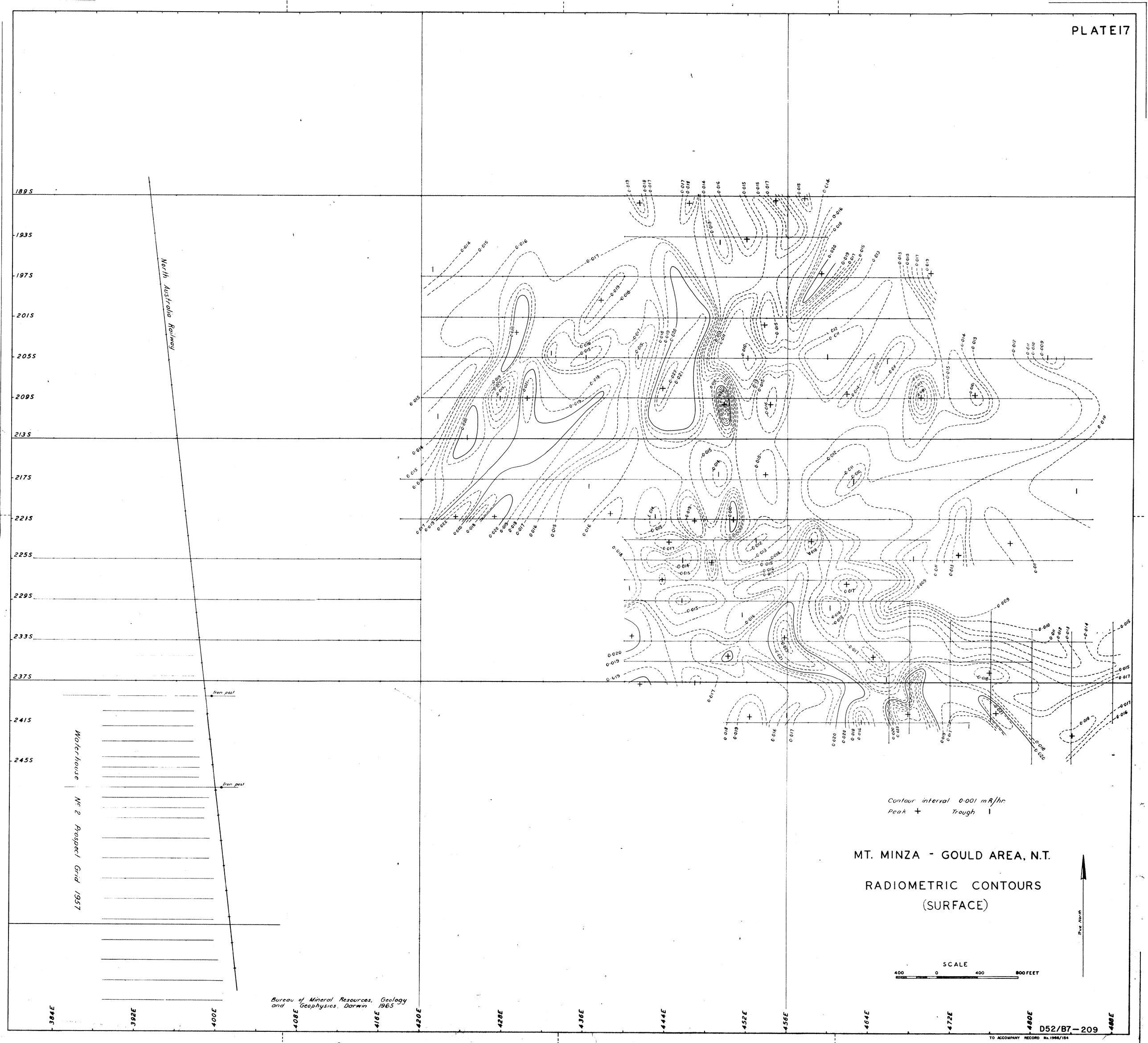

MT. MINZA - GOULD AREA, N.T.

RADIOMETRIC CONTOURS (SURFACE)

Bureau of Mineral Resources, Geology and Geophysics. Darwin 1965

D52/B7—209

TO ACCOMPANY RECORD No. 1966/154

PLATE 18

1

2

Imaginary %
+10
0
-10
-20

45°

Real %
110
100
90
80
70
60
50

Profiles derived from model experiments

Slingram

Imaginary %
+20
+10
0
-10
-20

Real %
140
120
100
80
60

L¹ Minimum depth of top
L² Maximum " " "
● Real current concentrations
o Imaginary current concentrations
P Outcrop of base of shale

Real component
Imaginary component

69°
37.5°

Traverse 237S
456E 58 60 62 64 66 68 70 72 74 76 478E

Turam A

Ratio
1·6
1·4
1·2
× 1·0
Cable (454E)

Phase °
+12
+8
+4
0
-4
-8
-12

Ratio
Phase

Turam B

Ratio
1·8
1·6
1·4
1·2
1·0

Phase °
+12
+8
+4
0
-4

Turam C

Ratio
1·6
1·4
1·2
1·0
0·8

Phase °
+12
+8
+4
0
-4
-8

× Cable

Scale
200 0 200 400 FEET

MT. MINZA - GOULD AREA, N.T.
ELECTROMAGNETIC PROFILES ON TRAVERSE 237S

Bureau of Mineral Resources, Geology and Geophysics, Darwin 1965

D52/B7-210
TO ACCOMPANY RECORD No. 1966/154

PLATE 19

Turam

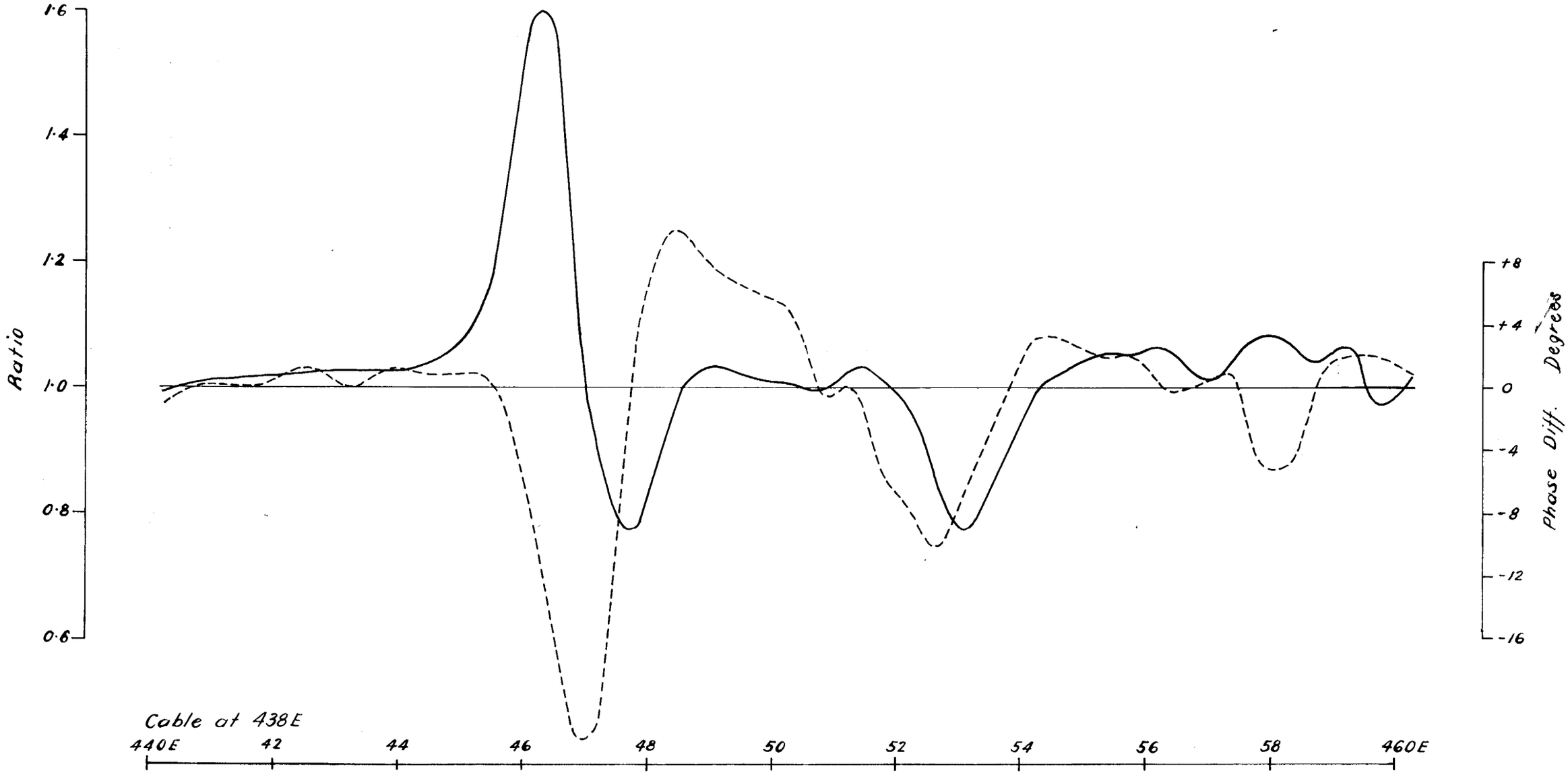

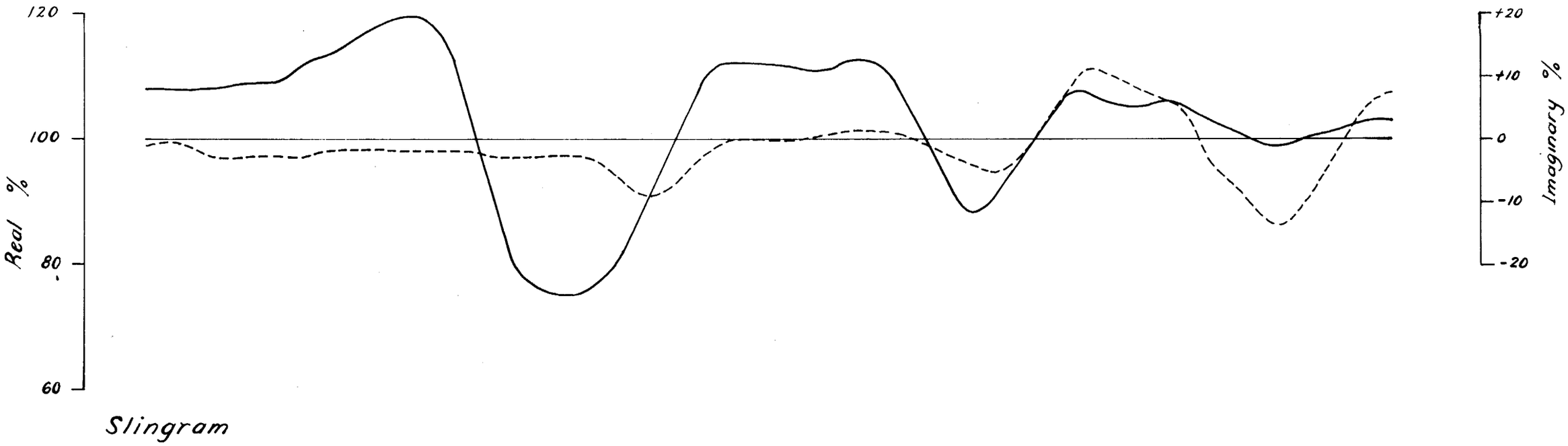

Slingram

MT. MINZA - GOULD AREA, N.T.

TURAM AND SLINGRAM PROFILES

——— Slingram real component
- - - - - - " imaginary component

——— Turam ratio
- - - - - - - " phase

Scale
200 0 200 400 FEET

Bureau of Mineral Resources, Geology and Geophysics, Darwin 1965

TO ACCOMPANY RECORD No. 1966/154

D52/B7 – 211

PLATE 20

1895
1935
1975
2015
2055
2095
2135
2175
2215
2255
2295
2335
2375
2415
2455

North Australia Railway

Waterhouse No 2 Prospect Grid 1957

iron post

iron post

.020

.020

.020

.020

.020

.020

.020

.020

.020

.020

.020

384E
392E
400E
408E
416E
420E
428E
436E
444E
452E
456E
464E
472E
480E
488E

Contours at .020 mR/hr

Bureau of Mineral Resources, Geology and Geophysics Darwin 1965

MT. MINZA - GOULD AREA, N.T.

RADIOMETRIC ANOMALIES DERIVED FROM SURFACE & SUBSURFACE DATA

True North

SCALE
400 0 400 800 FEET

D52/B7-212

TO ACCOMPANY RECORD No. 1966/154